MECHANISMS OF TELOMERASE REGULATION IN THE PROTOZOAN PARASITE, *TRYPANOSOMA BRUCEI*

by

Justin A. Davis

A dissertation submitted to the faculty of
The University of North Carolina at Charlotte
in partial fulfillment of the requirements
for the degree of Doctor of Philosophy in
Biology

Charlotte

2024

Approved by:

Dr. Kausik Chakrabarti

Dr. Shan Yan

Dr. Junya Tomida

Dr. Andrew W. Truman

Dr. Irina Nesmelova

ABSTRACT

JUSTIN A. DAVIS. The Role of Protein-Protein and RNA-Protein Interactions in Telomerase Regulation in the Protozoan Parasite, *Trypanosoma brucei*. (Under the direction of DR. KAUSIK CHAKRABARTI)

Telomeres are the DNA-protein complexes found at the ends of eukaryotic linear chromosomes. Telomeres pose a unique challenge to eukaryotic cells as they are unable to fully replicate their DNA all the way to the ends. If this problem is not resolved, cells would lose DNA after every cell division and telomeres would shorten. Over time this leads to significant telomere loss and genome instability. This issue is resolved by the ribonucleoprotein telomerase. Telomerase is the enzyme responsible for maintaining telomere length. The telomerase enzyme is composed of two main components: the telomerase reverse transcriptase protein, which catalyzes the extension of telomeric ends, and the telomerase RNA that provides the template for telomere synthesis. The telomerase RNA also forms a large structural scaffold upon which many accessory proteins can bind to form the complete telomerase holoenzyme. These interacting proteins and regulatory mechanisms are well studied in human, yeast and *Tetrahymena* systems. Telomerase interacting proteins and regulatory mechanisms have not been well studied in several ancient eukaryotes including clinically relevant human parasites like *Trypanosoma brucei* (*T. brucei*). *T. brucei* is a protozoan parasite that causes African sleeping sickness in humans. *T. brucei*, like many eukaryotic microbial pathogens, relies on constant high levels of telomerase activity to sustain the high proliferative capacity necessary to establish a successful infection in its human host. The aim of this dissertation is to highlight novel mechanisms of telomerase regulation in the ancient eukaryote, *T. brucei*. Chapter 1 is a published review synthesizing what is known about telomerase structure and regulation across model eukaryotes with emerging

views in parasitic protozoa. Chapter 2 describes a published study where we identified the first global interactome of telomerase in the bloodstream form *T. brucei* parasites using telomerase reverse transcriptase (TERT) as a bait in a mass spectrometry-based proteomics approach. Chapter 3 is an unpublished study where we identified the global interactome of the procyclic form *T. brucei* TERT and PTMs on semi-purified *T. brucei* telomerase using a mass spectrometry-based mapping approach. Chapter 4 describes an unpublished study where we studied the role of different structural domains in the *T. brucei* telomerase RNA and their relationship with the above interactors in telomerase RNA stability and telomerase catalytic activity.

DEDICATION

To my family
Without your constant love and support, I would not be where I am today

ACKNOWLEDGEMENTS

Firstly, I want to acknowledge and give all glory to God because he was the one who made all of this possible.

I want to thank all my family members epically my Mom and Dad for their constant love and support throughout my graduate school journey. They have always supported me and encouraged me to work hard and pursue my dreams.

I would like to thank my mentor Dr. Kausik Chakrabarti for everything he has done for me and my career throughout the ups and downs of this journey. You genuinely care for your students' success and are always willing to give your time and advice. I am grateful that you let me join your lab as an undergraduate when I had no idea what *T. brucei* or telomerase were and helped me grow and mature into the scientist I am today.

I would like to thank all my committee members Dr. Andrew Truman, Dr. Shan Yan, Dr. Junya Tomida and Dr. Irina Nesmelova. Thank you all for your direction and feedback throughout my graduate journey. Dr. Truman, thank you for all your insightful scientific advice and for making time and giving me great advice as I navigated graduate school and my next steps. Dr. Yan, thank you for your perspective and insightful questions that also pushed me to think about my own research more deeply. Dr. Tomida, thank you for your constant positive attitude and perspectives on my work. Dr. Nesmelova, thank you for agreeing to serve on my committee and bringing new angles and perspectives to my committee and my work.

Thank you to all past and present members of the Chakrabarti lab for their support along the way. Thank you to Dr. Abhishek Dey for training me when I first joined the lab and always pushing me to figure things out on my own and aiding my development as an independent

scientist. Thank you to Kaitlin Klotz and Tiffany Barwell for their constant friendship and support during my time in the Chakrabarti lab.

TABLE OF CONTENTS

LIST OF TABLES

LIST OF FIGURES

LIST OF ABBREVIATIONS

ANOVA-Analysis of variation
APC-Anaphase promoting complex
APC3-Anaphase promoting complex subunit 3
APEX-Ascobate peroxidase
ATR-Ataxia telangiectasia and Rad3-related protein
BF-Bloodstream form
CDC16-Cell cycle division control protein 16
CDC27-Cell cycle division control protein 27
CDC48-Cell cycle division protein 48
CTE-C-terminal extension
DDB1Damage specific DNA binding protein 1
DSB-Double-strand break
ES-Expression site
EXPIATR-Exponential isothermal amplification of telomere repeats
FDR-False discovery rate
HCD-High -energy collisional dissociation
HSP60-Heat shock protein 60
HSP70-Heat shock protein 70
HSP90-Heat shock protein 90
IP-Immunopurification
LFQ-Label free quantification
MKRN1-Makorin ring finger protein 1
NAT10N-acetyltransferase 10
NHEJ-Non-homologous end joining
NHP2-H/ACA ribonucleoprotein complex subunit 2
NOP1-Nucleolar protein 1
NOP10-Nucleolar protein 10
NOP56-Nucleolar protein 56
NOP58-Nucleolar protein 58
NOT1-General negative regulator of transcription subunit 1
PF-Procyclic form
PK-Pseudoknot
POT1-Portection of telomeres protein 1
PTM-Post-translational modifications
RAP1-Repressor/activator protein 1
RPA-Replication protein A
RRM-RNA recognition motif
SF3B1-Splicing factor 3B 1
SHAPE-Selective 2'-hydroxyl acylation analyzed by primer extension
TBE-Template boundary element
TCAB1-Telomerase cajal body protein 1

TCEP-Tris(2-caboxyethyl)phosphine
TEN-Telomerase N-terminal domain
TERT-Telomerase reverse transcriptase
TIF2-TRF-interactin factor 2
TIN2-TRF2-interacting nuclear protein 2
TLC1-Yeast telomerase RNA
TPC8-Telomerase positive control
TR-Telomerase RNA
*Tb*TR-*T.brucei* telomerase RNA
hTR-Human telomerase RNA
TRBD-Telomerase RNA binding domain
TRF1-Telomeric repeat binding factor 1
TRF2-Telomeric repeat binding protein 2
UMSBP2-Univerisal minicircle binding protein 2
VSG- Variant surface glycoprotein

CHAPTER 1: INTRODUCTION

Sections of this chapter have been published:

Davis, J. A., & Chakrabarti, K. (2022). Telomerase ribonucleoprotein and genome integrity—An emerging connection in protozoan parasites. *Wiley Interdisciplinary Reviews: RNA*, *13*(5), e1710.

1.1 Telomeres and Telomerase

Telomeres are the protective DNA-protein complexes found at the ends of eukaryotic chromosomes. Telomeres are maintained by the enzymatic activity of the ribonucleoprotein telomerase (Fig. 1A). Proper telomere maintenance is critical for the maintenance of genome integrity (Shay & Wright, 2019). In general, telomerase has two essential components: the telomerase RNA (TR), which contains a short template for telomeric DNA synthesis; and the catalytic protein telomerase reverse transcriptase (TERT) that catalyzes the extension of the telomere using TR as a template (Greider & Blackburn, 1989). There are a set of evolutionarily conserved proteins that bind to, and protect telomeric DNA inside of cells forming a structure known as the shelterin complex (Xin et al., 2008). The six main proteins that form the shelterin complex are—Telomere Repeat binding Factor 1 (TRF1), Telomere Repeat binding Factor 2 (TRF2), Protection of telomere 1 (POT1), Repressor/Activator protein 1 (RAP1), TRF1-and TRF2-Interacting Nuclear Protein 2 (TIN2), and TPP1 (Xin et al.,2008). The shelterin complexes' role is to protect telomeres from degradation inside the cell and to prevent the cell from recognizing telomeres as DNA damage.

The core protein component of the telomerase holoenzyme is the TERT. The minimum components required for telomerase activity are TERT and TR. TERT is the most highly conserved component of the telomerase holoenzyme across a range of species and uses its reverse transcriptase activity to extend telomeres (Kumar et al., 2018). The TERT protein is composed of four domains: Telomerase “essential” N-terminal (TEN) domain, TR binding domain (TRBD), Reverse Transcriptase (RT) domain and C-Terminal Extension (CTE) also known as the Thumb domain that are conserved across eukaryotes (Fig. 2).

The TR provides the template that the TERT protein uses to catalyze the extension of telomeres (Greider and Blackburn, 1989). The TR forms a large structural scaffold for the binding of accessory proteins that form the complete telomerase holoenzyme. Unlike the TERT, TR is highly divergent across species, differing in size, sequence and structure (Fig. 3). The smallest TR was reported in ciliates, and was found to be around 150–200 nucleotides (nt) long (Amanda & Romero, 2002). Vertebrate TRs generally range from 310 to 560 nt long while yeast TRs range between 780 and 1820 nt long (Gunisova et al., 2009; Xie et al., 2008). Non-yeast fungal TRs have also been identified and studied and were found to be over 2000 nt in length (Qi et al., 2013). Plant TRs are closer to the size of ciliate and vertebrate TRs and generally range from 200–300 nt long (Song et al., 2019). These significant size variations demonstrate the diversity of TR length across eukaryotes. The TR contains several key structural domains: Template region, Template Boundary Element (TBE), Pseudoknot (PK) and the Stem Terminus Element (STE) (Helix IV in kinetoplastid TR) (Dey & Chakrabarti, 2018; Egan & Collins, 2012a; Podlevsky et al., 2016). In vertebrate TR, the homologous domain to kinetoplastid Helix IV is called the CR4/5 domain (Chen et al., 2000; Kim et al., 2014). The Helix IV (CR4/5) domain is a broadly conserved domain across a variety of eukaryotic clades. The template is a

single stranded region in the TR that hybridizes with telomeric DNA (Greider, 1991). The TERT protein will use this sequence in the template region to add telomeric repeats and extend telomeric DNA sequences. The template region and key TR structural domains, required for catalytic activity, form a conserved region in the TR called the 'catalytic core'.

1.2 Telomerase Interactions

The minimum requirements for telomerase activity *in vitro* are the TERT protein and its corresponding TR molecule (Masutomi et al., 2000). The TR molecule forms a large structural scaffold upon which many accessory proteins can bind to form the complete telomerase holoenzyme *in vivo*. These interacting proteins have been extensively characterized in *Tetrahymena*, yeast and mammalian systems. These accessory proteins are important for the activity and regulation of telomerase in living organisms. Given that the TR molecule is the most divergent component across species, the interacting partners of telomerase change depending on the species examined (Wang et al., 2019). In *Tetrahymena thermophila* (*T. thermophila*), a free-living ciliate, a combination of electron microscopy (EM) and cryogenic EM (cryo-EM) reconstruction of the telomerase complex revealed many accessory protein interactors including: p65, p75, p45, p19, p50, Teb1, Teb2, and Teb3 (Table1) (Jiang et al., 2015; Jiang et al., 2013). The holoenzyme components, p75, p19, and p45 form a sub complex. While p65 has a direct interaction with *Tetrahymena* telomerase RNA (*Te*TR), the p75-p45-p19 subcomplex is connected to TERT-TR-p65 core by a bridging interaction with p50. These proteins have been shown to be required for telomerase stability and activity (Witkin & Collins, 2004). Teb1-Teb2-Teb3 are paralogs of the single-stranded DNA (ssDNA) binding protein replication protein A (RPA) from mammalian cells. RPA is a major player in a variety of cellular DNA repair

pathways and serves to bind ssDNA and activate the ATR kinase (Choi et al., 2010). These proteins also form a sub complex and are required for the stability of the telomerase holoenzymes interaction at telomeres (Jiang et al.,2015). The cryo-EM structure of the yeast telomerase holoenzyme remains to be solved but interacting partners of telomerase in yeast have been identified through genetic studies, mass spectrometry analysis and other biochemical methods. The interacting proteins identified to date include: Pop1, Pop6, Pop7, Est1, Est3, Ku 70/80, Smd2, Smb1, and Smd3 forming the Sm7 complex (Lemieux et al., 2016; Wang et al., 2019). Telomere replication proteins Est1 and Est3 are required for telomerase activity. The exact function of Est1 is unknown and it is not homologous to any other known telomerase associated protein. Est1 interacts with the TR directly via an RNA recognition motif (RRM), but it has also been shown that Est1 can bind to telomeric DNA. Est1 functions to tether yeast telomerase to telomeres (Evans & Lundblad, 2002; Zhou et al., 2000). Est3 is required for telomere replication and it has been shown to be involved in the unwinding of RNA/DNA duplexes to allow for telomere elongation by telomerase (Sharanov et al., 2006). The *Saccharomyces cerevisiae* (*S. cerevisiae*) TR, TLC1 contains a P3 like domain that is similar to P3 domains found in RNase P/MRP. This P3-like domain in TLC1 functions as the binding site for the Pop6/7 heterodimer and the Pop1 protein. Pop6/7 and Pop1 are required for telomerase activity by stabilizing the TLC1 molecule as well as stabilizing Est1 and Est3 interactions in the telomerase holoenzyme (Lemieux et al.,2016). The Ku70/80 heterodimer participates in the DSB repair pathway via- nonhomologous end joining (NHEJ). Ku70/80 has been shown to bind with TLC1 and knockout of Ku70/80 lead to progressive telomere shortening in *S. cerevisiae*. Ku70/80 interaction with TLC1 enables telomerase to act at both broken and normal chromosome ends (Stellwagen et al., 2003). Small nuclear proteins, Smd1, Smd2, and Smd3 are

involved in pre-mRNA splicing and bind to a conserved Sm binding site on small nuclear RNA (snRNA) molecules (Rymond, 1993). These proteins bind to TLC1 at the 3’ end and form the Sm7 complex. This complex is required for the processing of TLC1 including, 5’-capping and 3’-end processing, and essential for telomerase activity and stability (Vasianovich et al., 2020).

The cryo-EM structure of human telomerase has been solved. This cryo-EM analysis along with previous mass spectrometry analysis identified several accessory proteins that form the human telomerase holoenzyme. These proteins are: Dyskerin, NHP2, GAR1, NOP10, and TCAB1 (Cohen et al., 2007; Nguyen et al., 2018). The human telomerase RNA (hTR) contains an H/ACA box small nucleolar RNA (snoRNA) domain. Dyskerin, NHP2, GAR1, and NOP10are all H/ACA box binding proteins that interact with the hTR by interacting with the H/ACA consensus sequences. These H/ACA core proteins are required for the processing of hTR and telomerase biogenesis in vivo (Nguyen et al.,2018). The mutations in dyskerin and other holoenzyme components, can lead to telomere shortening disease in humans, such as, dyskeratosis congenita (Vulliamy et al., 2001). TCAB1 is a component of the telomerase holoenzyme and required for telomerase activity via an RNA activity switch, where TCAB1 can control regional folding in the hTRCR4/5 domain to regulate telomerase activity in vivo (Chen et al., 2018). TCAB1 has also been shown to be required for telomerase localization and recruitment to telomeres. Specifically, TCAB1 is required for telomerase accumulation in cajal bodies (Venteicher et al., 2009).

In human parasites, interacting partners of telomerase have not been extensively characterized through cryo-EM or mass spectrometry analyses. Extensive characterization of protein interactors in human parasites could provide novel insight of RNA and protein coevolution and telomerase regulation in deep branching eukaryotes.

1.3 *Trypanosoma brucei* Biology

Trypanosoma brucei (*T. brucei*) is a parasitic protozoan that causes a disease called African trypanosomiasis, also known as African sleeping sickness in humans. The phylogeny of *T. brucei* parasites is quite complex and there are three distinct subspecies of *T. brucei*. The three subspecies are: *Trypanosoma brucei gambiense*, *Trypanosoma brucei rhodesiense* and *Trypanosoma brucei brucei*. *Trypanosoma brucei brucei* does not infect humans and causes a disease in cattle and other livestock called nagana. *Trypanosoma brucei gambiense* and *Trypanosoma brucei rhodesiense* are the subspecies responsible for causing African sleeping sickness in humans (Steverding, 2017). African sleeping sickness is a vector borne disease that is common in sub-Saharan Africa where the insect vector, the Tsetse fly (*Glossina spp*.) is ubiquitous. *T. brucei* parasites have a two-host life cycle where they shuttle between vertebrate and invertebrate hosts (Fig. 2B). In the insect vector, the parasite differentiates into a developmental stage called the procyclic form. When the parasites are in their mammalian hosts, they differentiate into another developmental stage called the bloodstream form. The bloodstream form of the parasite is responsible for causing the symptoms of African sleeping sickness.

The symptoms of African sleeping sickness in its early stages can appear to be flu like symptoms and they include: fever, headaches, and joint pain. In the later stages of the disease, the parasite has spread to the nervous system and you start to have manifestations of various neurological symptoms like: behavioral changes, confusion and poor coordination (Welburn et al., 2001). There is no cure for African sleeping sickness and the disease is always fatal if left untreated and the current drug treatments suffer from high toxicity and varying side effects

(Kennedy, 2013). To compound these issues, there is also no vaccine available to prevent the transmission of this disease in its endemic regions. Taken together, these problems highlight the importance of studying the basic biology of *T. brucei* parasites to glean knowledge that may be instrumental in the development of new therapeutics for the treatment of African sleeping sickness.

1.4 Telomerase in *Trypanosoma brucei*

In eukaryotic phylogeny, Kinetoplastids (e.g. *T. brucei*) represent a unique clade of lower eukaryotes exhibiting extraordinary features of RNA metabolism, such as trans-splicing (Sutton & Boothroyd, 1986), polycistronic transcription (Respuela et al., 2008), and RNA editing (Simpson et al., 2000). Remarkably, the kinetoplastid parasite *T. brucei* telomerase RNA (*Tb*TR) has several unique features that suggest a mechanistically different process of telomerase-mediated telomere maintenance in the flagellates compared to yeast, mammalian, and Tetrahymena models (Gupta et al., 2013; Podlevsky et al., 2016; Sandhu et al., 2013). The *Tb*TR gene was found to be present on chromosome 11 and encode an approximately 900 nt long transcript transcribed by RNA polymerase II (Gupta et al., 2013; Sandhu et al., 2013). This size is like yeast but certainly larger than vertebrate TRs. The *Tb*TR was found to be processed through an RNA maturation process called trans-splicing. This process leads to the addition of a 50 nt spliced leader (SL) RNA sequence to the 5’ ends of the mature *Tb*TR transcript. The average length of telomeres in *T. brucei* Lister 427 strain is approximately 15 kB long (Dreesen & Cross, 2008). The deletion of *Tb*TR leads to progressive telomere shortening at a rate of approximately 3–5 bp every generation (Sandhu et al., 2013). This result demonstrated the requirements of the TR for telomere synthesis in *T. brucei*. The secondary structure model of

*Tb*TR suggests that the template domain is single stranded, which would allow it to bind to telomeres and provide the necessary template for telomere synthesis (Podlevsky et al., 2016; Sandhu et al., 2013). To further validate that the *Tb*TR provides the template for telomere synthesis *in T. brucei*, mutations were introduced in the template domain of the *Tb*TR, and it was observed that the corresponding mutations were incorporated into telomeric repeat sequences (Sandhu et al., 2013). This confirmed that the *Tb*TR provides the critical templating function that controls telomere synthesis in *T. brucei*. In addition to having a unique, ciliate-like shorter stem-loop at the 3' end of the template instead of a typical PK domain (Podlevsky et al., 2016; Sandhu et al., 2013), the 5' and 3' ends of the *Tb*TR contain consensus sequences of C and D box domain, which is a hallmark of C/D box snoRNAs (Gupta et al., 2013). A computational model (Gupta et al., 2013) of *Tb*TR suggests that the C and D consensus sequences partially bind with each other. It was also demonstrated that NOP58, a protein of the C/D snoRNA family, binds to *Tb*TR (Gupta et al., 2013). The presence of a novel C/D box domain in *Tb*TR suggests a mechanistic difference in the processing and biogenesis of *Tb*TR compared to higher eukaryotes whose TRs contain an H/ACA box domain.

The protozoan parasite *T. brucei* completes its life cycle through discrete developmental stages, providing a potentially undiscovered pocket of distinct mechanisms of the regulation of stage-specific telomerase activity. The population doubling (PD) time between the two proliferative stages of *T. brucei*, the bloodstream form (BF, mammalian infective stage) and procyclic form (PF, insect stage) are significantly different, for example, the PD of BF cells is shorter (6.5 h) than that in PF cells (12–24 h) in laboratory culture conditions. However, the relationship between the *T. brucei* PD and telomerase activities in different life cycle stages are yet to be determined. Considering the phylogenetic diversity of TR functional domains, this

flagellate TR from *T. brucei* contains two distinct structural domains that are required for the reconstitution of telomerase activity (Podlevsky et al., 2016). Like yeast and metazoan TRs, these domains are located about 350 nt apart within the RNA. Whether the in-cell structural and functional properties of *Tb*TR show stage-specific differences, owing to differences in telomerase activity, would be of considerable interest. Because of this, it is possible that *T. brucei* could show novel TR folding, telomerase activity, and changes in the rate of telomere synthesis. Indeed, our recent experiments utilizing selective 20-hydroxyl acylation analyzed by primer extension and mutational profiling (SHAPE-MAP) to investigate *Tb*TR folding in the BF and PF stages, revealed developmental differences in the *Tb*TR structure (Dey et al., 2021) (Fig. 4). This stage-specific RNA structural rearrangement within telomerase RNP in *T. brucei* influences telomerase activity and could potentially regulate PD and chronicity of parasite infection.

1.5 Figures

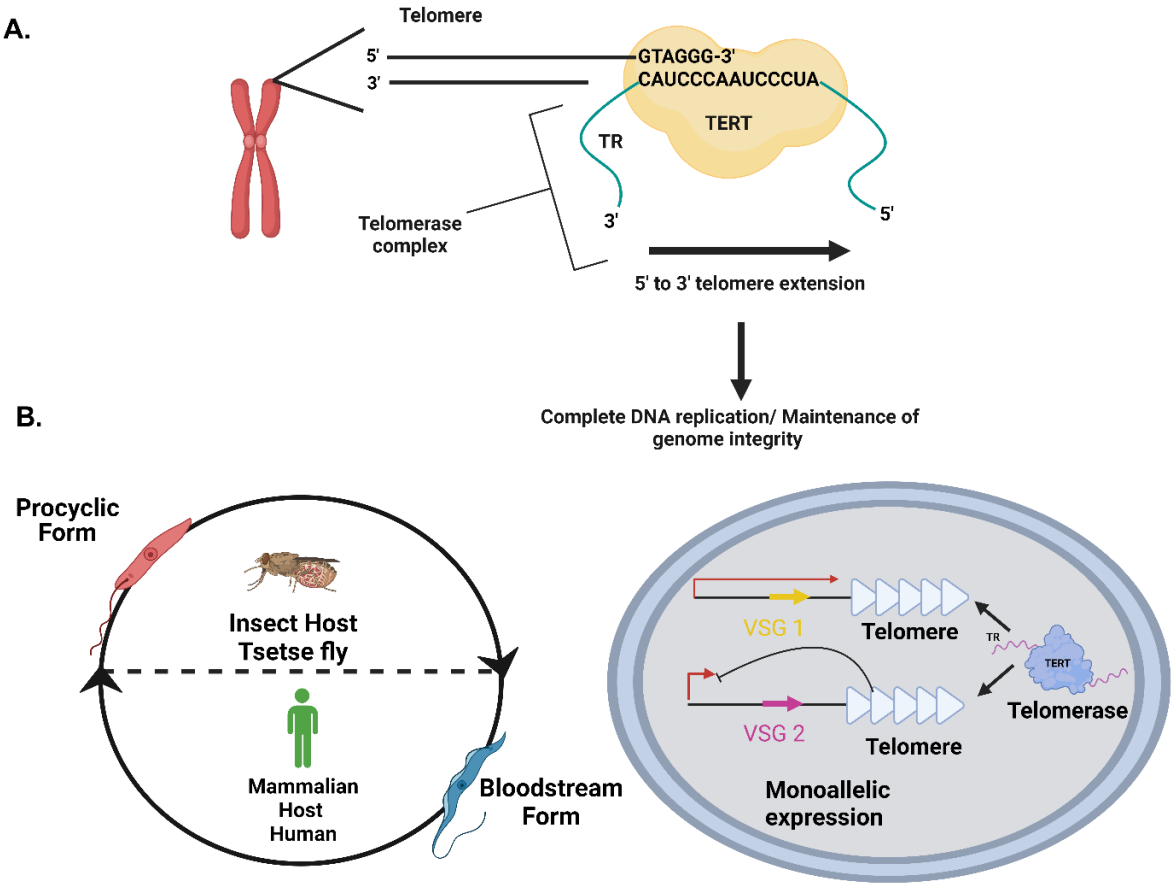

Figure 1. Telomere-telomerase complex in eukaryotes and *T. brucei* biology. (A) Telomere-telomerase complex in eukaryotes. (B, left) Life cycle of *T. brucei* highlighting the two proliferative stages that can be easily cultured in the lab. (B, right) Structure of subtelomeric virulence genes in *T. brucei*. *T. brucei* uses antigenic variation to alter VSG expression to evade host immune responses. Telomerase activity is required to maintain the integrity of subtelomeric virulence genes.

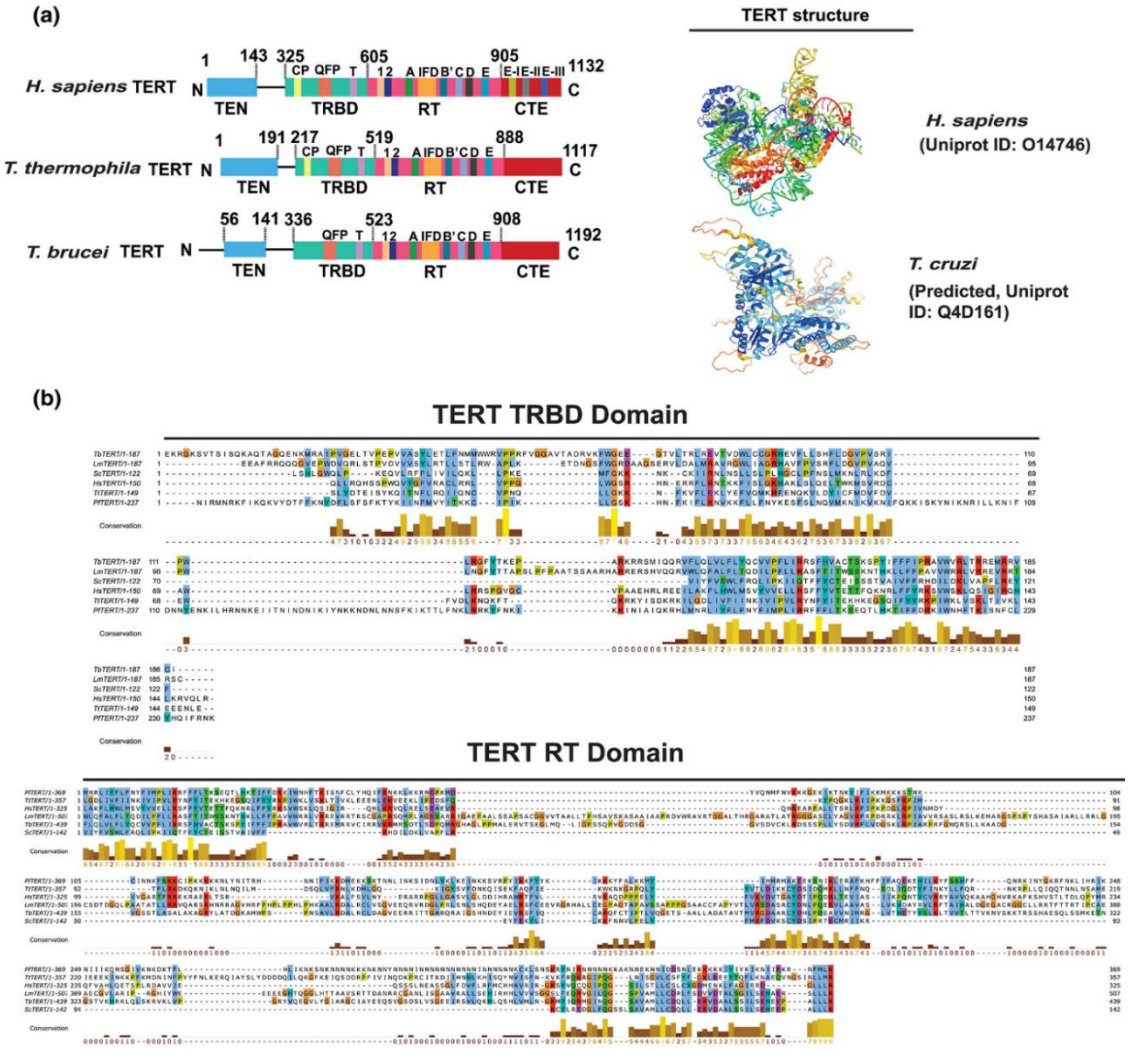

Figure 2. TERT domain distribution and sequence alignment across eukaryotes. (a). Schematic of TERT protein showing conserved domains and motifs in *H. sapiens*, *T. thermophila*, and *T. brucei*. TERT structures from *H. sapiens* and predicted TERT structure from *Trypanosoma cruzi* (*T. cruzi*) obtained by AlphaFold (Jumper et al., 2021). The cryo-EM structure of *H. sapien* TERT was obtained from Nguyen et al., 2018. Dark blue represents a very high model confidence (pLDDT >90), light blue confident (90 >pLDDT >70), yellow low confidence (70 >pLDDT >50), orange very low confidence (pLDDT <50). (b). Sequence alignment showing the conserved reverse transcriptase (RT) and telomerase RNA binding (TRBD) domains in representative species. Conserved residues of TERT between *T. brucei*, *L. major*, *S. cerevisiae*, *H. sapiens*, *T. thermophila*, *and P. falciparum* are shown for both domains. The sequence alignment was performed using a combination of MUSCLE and Jalview. Dots between sequence alignments represent deletions of residues/regions across species. Bars at the bottom represent the degree of conservation of given amino acid residues. Amino acids are colored based on their chemical properties blue-hydrophobic, red-positively charged, magenta-negative charge, green-polar, pink-cysteines, orange-glycine's, yellow-prolines, cyan-aromatic, and white-nonconserved

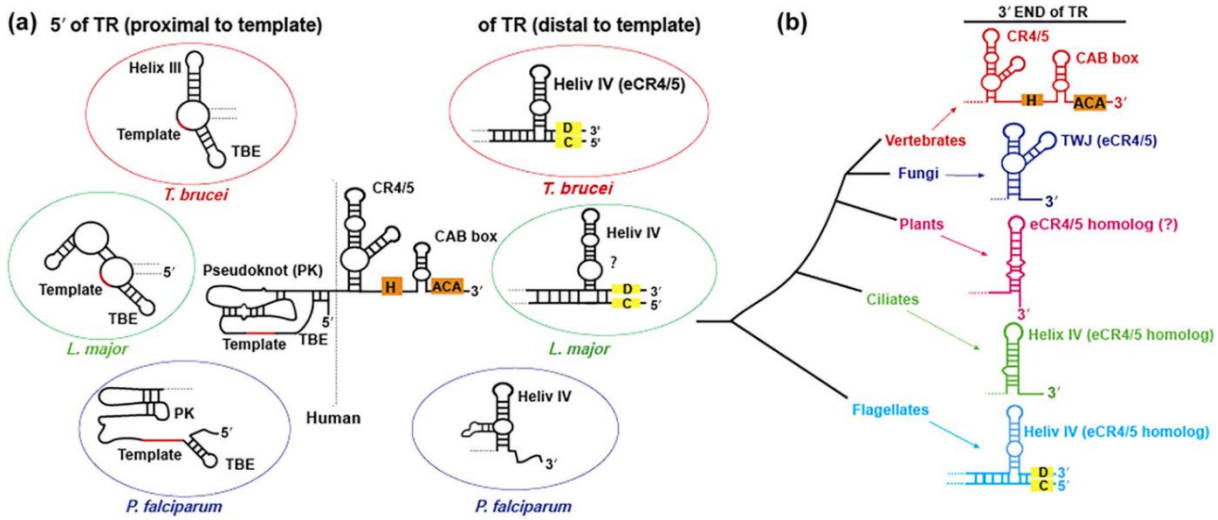

Figure 3. Structural diversity of telomerase RNAs across eukaryotes. (a). Telomerase RNA secondary structure in parasitic protozoa. Secondary structure of telomerase RNA catalytic core from *T. brucei*, *L. major* (predicted), and *P. falciparum* (predicted). The 5′ end of the telomerase RNA contains important structural domains required for telomerase activity termed the catalytic core. The 3′ end of the telomerase RNA contains domains required for telomerase RNA biogenesis including C/D snoRNA domains present in *T. brucei* and *L. major*. (b). Simplified phylogeny showing the structural variation of the 3′ end of telomerase RNA in represented eukaryotic clades. A conserved Helix IV (eCR4/5) domain is present in the representative taxa. The CR4/5 domain is not universally conserved in metazoans. It is only present in vertebrates and lower metazoans (Logeswaran et al., 2021). In plants, a 3′ TR domain was found to stimulate in vitro telomerase activity along with template pseudoknot (Song et al., 2019), like CR4/5 in vertebrates, but this structure is yet to be fully characterized. Flagellate telomerase RNA contains a C/D snoRNA domain and the mammalian telomerase RNA contains a H/ACA box snoRNA domain. The presence of a C/D box domain in flagellate telomerase RNA represents a divergence in the biogenesis pathway of the telomerase RNA in deep branching eukaryotes.

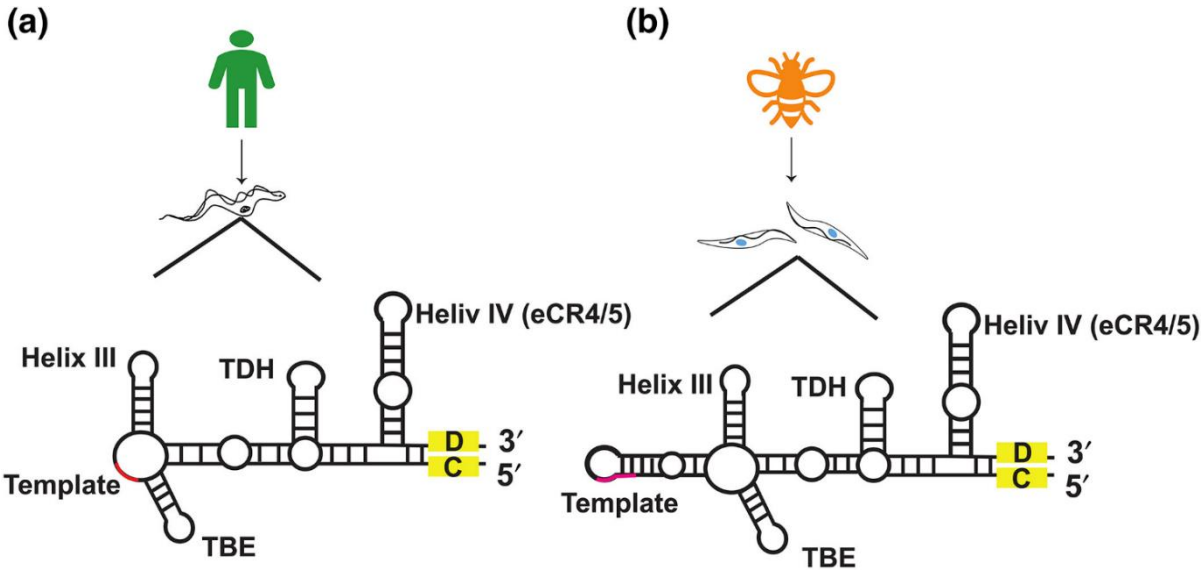

Figure 4. Developmental differences in *T. brucei* telomerase RNA secondary structure. (a). Bloodstream form (BF) *T. brucei* telomerase RNA secondary structure highlighting key structural elements. (b). Procyclic form (PF) *T. brucei* telomerase RNA secondary structure highlighting key structural elements. The main structural changes occurring are in the template region of the telomerase RNA between the two developmental stages. The structural rearrangements of the *T. brucei* telomerase RNA was determined by mutational profiling and high-throughput sequencing (Dey et al., 2021).

CHAPTER 2: PROTEOMIC ANALYSIS DEFINES THE INTERACTOME OF TELOMERASE IN THE PROTOZOAN PARASITE, *TRYPANOSOMA BRUCEI*

This chapter has been published:

Davis, J. A., Reyes, A. V., Saha, A., Wolfgeher, D. J., Xu, S. L., Truman, A. W., ... & Chakrabarti, K. (2023). Proteomic analysis defines the interactome of telomerase in the protozoan parasite, Trypanosoma brucei. *Frontiers in Cell and Developmental Biology*, *11*, 1110423.

2.1 Introduction

Telomeres are the nucleoprotein structures found at the ends of eukaryotic chromosomes. Conventional DNA polymerases are unable to fully replicate the ends of linear DNA molecules, which leads to progressive telomere shortening after every cell division (Shay and Wright, 2019). This problem is solved by the ribonucleoprotein enzyme, telomerase. Proper maintenance of the telomeric end is critical for maintaining genome integrity in eukaryotes. The telomerase enzyme has two essential components: the telomerase RNA (TR), which provides the template required for telomeric DNA synthesis (Greider and Blackburn, 1989); and the catalytic protein telomerase reverse transcriptase (TERT) that catalyzes the de novo synthesis of the telomere G-rich strand. The action of telomerase counteracts progressive telomere shortening after every cell division.

TERT and TR are the minimum components required for the telomerase activity *in vitro.*

(Chen et al., 2000; (Collins, 2006). TR can form a large structural scaffold upon which many accessory proteins can bind to and form the complete telomerase holoenzyme *in vivo*.

These accessory proteins are required for *in vivo* telomerase activity and regulation (Wang et al., 2019). Interacting partners of the TERT protein have been extensively characterized in yeast, human, and Tetrahymena systems, but they have not been extensively studied in parasitic protozoa including clinically relevant human parasites, such as *Trypanosoma brucei* (*T. brucei*). *T. brucei* is the parasite that causes African sleeping sickness in humans. During its life cycle, *T. brucei* will shuttle between an insect vector and a mammalian host. During this time, the parasite will differentiate into distinct developmental stages: Bloodstream form (BF) parasites proliferate in the mammalian host, and Procyclic form (PF) parasites proliferate in the midgut of the insect vector. Unlike human somatic cells, which tightly regulate telomerase activity, *T. brucei* telomerase is constantly active, enabling continued cell division in their hosts, leading to a chronic infection. BF *T. brucei* also has the advantage of evading its host immune response through antigenic variation. During this process, *T. brucei* regularly switches to express different Variant Surface Glycoproteins (*VSGs*), its major surface antigen. *T. brucei* has a very large *VSG* gene pool, but only one *VSG* gene is expressed at any given time. *VSG*s are expressed exclusively from *VSG* expression sites (ESs), which are large polycistronic transcription units located at subtelomeric loci of the parasite's genome within 2 kb of telomeres (De Lange & Borst, 1982). Therefore, telomerase activity is critical to maintain the integrity of these *VSG* genes (Fig 1B). In cells where the TERT protein has been deleted *(Tb*TERT−/−), extremely short telomeres adjacent to the active ES leads to an increase in *VSG* switching frequency (Dreesen & Cross, 2006; Hovel-Miner et al., 2012). Telomeric binding proteins have also been shown to affect *VSG* silencing and switching (Afrin et al., 2020; Benmerzouga et al., 2013; Jehi et al., 2016; Jehi et al., 2014; Nanavaty et al., 2017; Rabbani et al., 2022; Yang et al., 2009). Telomerase mediated

telomere maintenance in *T. brucei* is required for the maintenance of subtelomeric *VSG* genes. Because of this, studies of telomerase function and regulation in *T. brucei* could give novel insights into the pathogenicity of this parasite.

The RNA component of *T. brucei* telomerase (*Tb*TR) has a unique structure and sequence composition compared to higher eukaryotes (Sandhu et al., 2013; Podlevsky et al., 2016; Dey et al., 2021). Our recent study on *Tb*TR suggests mechanistic differences in telomere maintenance between *T. brucei* and higher eukaryotes (Dey et al., 2021; Rabbani et al., 2022) underscoring the importance of investigating the functional interactome of *T. brucei* telomerase. Previous proteomic studies on ciliated single-cell protozoan Tetrahymena identified several RNA binding proteins, including p65 that copurifies with TR and TERT and promotes proper folding of TR for telomerase holoenzyme assembly and activity (Berman et al., 2010; He et al., 2021; Singh et al., 2012; Upton et al., 2017; Witkin & Collins, 2004). Although homologs of p65 have not been found outside ciliate ancestry, the complex of dyskerin, NHP2, NOP10, and GAR1 that bind the H/ACA domain of human TR are thought to be the functional analog of the p65 chaperone in human telomerase (Berman et al., 2010; Roake & Artandi, 2020). Indeed, these H/ACA binding proteins are known to facilitate human TR folding by enabling the human CR4/5 domain to adopt a particular conformation that interacts with TERT (Chen et al., 2018; Egan and Collins, 2012). Interestingly, in *Tb*TR, the human H/ACA type snoRNP binding domain is replaced by a unique C/D box snoRNA domain (Gupta et al., 2013). In addition, TCAB1, another telomerase RNA-binding protein, was previously discovered as a part of human telomerase complex by mass spectrometry, which is important for intracellular trafficking (Venteicher et al., 2009) and regulating the folding of CR4/5 domain of human TR and telomerase

activation. However, even though *Tb*TR possesses stage-specific structural changes in an active telomerase complex (Dey et al., 2021), major interactors in this complex remain unidentified.

In addition to the canonical function of the TERT protein to protect telomeric ends of chromosomes, emerging evidence also suggests that telomerase can contribute to oxidative stress response in a telomere-independent manner. TERT has been shown to shuttle to mitochondria under increased oxidative stress and influence processes related to DNA damage and cell death (Indran et al., 2011; Santos et al., 2004). There are 5 respiratory chain complexes in human mitochondria that can regulate redox processes and hTERT enhances complex I activity (Ale-Agha et al., 2021). Beyond this, very little is known about the involvement of mitochondrial proteins in TERT function. Interestingly, *T. brucei* protein *Tb*UMSBP2 (Klebanov-Akopyan et al., 2018), which binds to single stranded G-rich sequence at the replication origins of the mitochondrial DNA of trypanosomatids, colocalizes with telomeres at the nucleus, but whether this activity is coordinated by telomerase mediated DNA repair is not known.

To gain a global view and mechanistic insight into telomerase function and regulation in *T. brucei*, we identified the interacting factors of *T. brucei* telomerase reverse transcriptase (*Tb*TERT) expressed in the Bloodstream Form (BF) cells using an affinity-purification based mass spectrometry approach. We identified previously known and novel interactors of *Tb*TERT and validated several key interactions. Studying the interactome of *Tb*TERT lays the foundation for future studies of telomerase regulation in *T. brucei*.

2.2 Materials and Methods

Culture of bloodstream form (BF) T. brucei cells

T. brucei Lister strain 427 was used throughout this study. All BF cells were grown in HMI-9 media supplemented with 10% heat inactivated Fetal Bovine Serum (FBS) at 37°C and 5% CO2. *T. brucei* Lister 427 strain expressing the T7 polymerase and Tet repressor (single marker, AKA SM) (Wirtz et al., 1999) was grown in media containing 2 μg/mL of G418; *Tb*TERT-FLAG-HA-HA (F2H) cells grown with 2 μg/mL of G418, 0.1 μg/mL Puromycin; *Tb*TR ΔC/D box mutant cells were grown with 2 μg/mL of G418, 4 μg/mL of Hygromycin, 2.5 μg/mL of Phleomycin, 5 μg/mL of Blasticidin, 0.1 μg/mL of Puromycin and 0.1 μg/mL of Doxycycline to constitutively induce the *Tb*TR mutations.

Plasmids

The *Tb*TR WT gene without 3' C/D box region (nt 841–943) together with 400 bp upstream and 380 bp of downstream *Tb*TR flanking sequences were cloned into the pLew111 plasmid to generate pLew111-*Tb*TR ΔC/D box plasmid.

Generation of the BF T. brucei ΔC/D box mutant strain

To generate the *Tb*TR ΔC/D box mutant strain, pLew111-*Tb*TR ΔC/D box plasmid (nt 841–943 deleted) was digested with NotI and targeted to an rDNA spacer in the SM/*Tb*TR−/− cells under the phleomycin selection. Clones were confirmed by northern analysis. XhoI digested pSK-*Tb*TERT-3C-FLAG-HA-HA-PUR plasmid (Dey et al., 2021) was subsequently transfected into the same cells under the puromycin selection to generate the SM/TbTR ΔC/D box/ *Tb*TERT+ / F2H strain. Clones were confirmed by western and Southern blotting.

Immunopurification of T. brucei telomerase complexes

Immunoprecipitation of *T. brucei* telomerase was performed using a custom made anti-*Tb*TERT antibody (Dey et al., 2021) to purify native telomerase complexes from BF Wild-type (WT) and BF *Tb*TR ΔC/D box cells. Approximately, 5 × 108 cells/300 mL were collected by centrifugation at 1900 RPM for 6 min. Following centrifugation, cells were lysed by homogenization in 500 µL of 1X immunopurified (IP) lysis buffer (25 mM Tris-HCl pH 7.5, 150 mM KCl, 1 mM EDTA, 10 mM MgCl2, 12% glycerol, 0.5% IGEPAL CA630, 1X protease cocktail inhibitor, and 20 units of Ribolock RNase inhibitor). Lysate was then cleared of cell debris by centrifugation at 3000 RPM for 5 min at 4°C. The lysate was then pre-cleared by incubated with 50 µL of pre-washed Dynabeads protein G (10003D) for 1 h at 4° C on rotation. Pre-cleared lysates were then incubated overnight at 4°C on rotation with 5 µg of a custom anti-*Tb*TERT antibody and an IgG antibody was added to the control (Dey et al., 2021). The next day, 50 µL of pre-washed Dyna beads protein G was added to the lysate antibody mixture and incubated at 4°C for 2 h on rotation. After incubation, the beads were collected in a magnetic stand and washed twice in ×1 IP lysis buffer. After washing, the bound protein was eluted off the beads by boiling in 100 µL of 1X SDS-PAGE dye for 5 min at 95° C. Eluted proteins were then stored in −80° C until further use. Each experiment was performed in biological triplicate (3 IPs and 3 IgG controls). Bound complexes were assayed for the presence of *Tb*TERT by using an anti-FLAG antibody as the BF WT cells were *Tb*TERT-FLAG-HAHA tagged. Briefly, 4 µL of 100 µL of sample was loaded onto 4%– 12% Novex Tris-glycine gel (Invitrogen, XP04120BOX). Western blotting was done using an anti-FLAG antibody, diluted 1:500, and the VeriBlot for IP Detection Reagent (HRP, ab131366) diluted to 1: 10,000. Detection was then

done using Pierce ECL Plus Chemiluminescence kit (Thermo Fisher Scientific, 32,106). Imaging was then done using Bio-Rad ChemiDoc MP system.

Immunopurification was also performed using Pierce AntiDYKDDDDK magnetic beads (A36797). Approximately 6 × 108 cells/300 mL were harvested and lysed in 300 μL of immunopurified (IP) lysis buffer (25 mM Tris-HCl pH 7.5, 150 mM KCl, 25 mM NaCl, 1 mM EDTA, 10 mM MgCl2, 0.5% IGEPAL CA630, 1× protease cocktail inhibitor and 20 units of Ribolock RNase inhibitor). Lysate was cleared of debris by centrifugation at 3,000 rpm for 5 min at 4°C and incubated with pre-washed 50 μL of Pierce Anti-DYKDDDDK magnetic beads (A36797) at 4°C for 2 h with rotation. Following incubation, the beads were washed twice by ice cold IP buffer and once with ice cold DEPC water. The beads were then resuspended in 50 μL of RNAse free water.

LC-MS/MS analysis

Proteins were separated by SDS-PAGE and Gel segments were cut and subjected to in-gel digestion using trypsin. Peptides were desalted using C18 ZipTips (Millipore). Peptides were analyzed on a Q-Exactive HF hybrid quadrupole-Orbitrap mass spectrometer (Thermo Fisher) equipped with an Easy LC 1200 UPLC liquid chromatography system (Thermo Fisher). Peptides were first trapped using trapping column Acclaim PepMap 100 (75 uM x 2 cm, nanoViper 2Pk, C18, 3 μm, 100A), then separated using analytical column Acclaim PepMap RSLC (75 um × 25 cm, nanoViper, C18, 2 μm, 100A) (Thermo Fisher). The flow rate was 300 nL/min, and a 120-min gradient was used. Peptides were eluted by a gradient from 3% to 28% solvent B (80% (v/v) acetonitrile/0.1% (v/v) formic acid) over 100 min and from 28% to 44% solvent B over 20 min, followed by a short wash at 90% solvent B. For DDA acquisition, the precursor scan was from

massto-charge ratio (m/z) 375 to 1,600 and the top 20 most intense multiply charged precursors were selected for fragmentation. Peptides were fragmented with higher-energy collision dissociation (HCD) with normalized collision energy (NCE) 27.

LC-MS/MS data and statistical analysis

The resulting raw data files were searched against a concatenated library (*Tbrucei*TREU927 release 32 databases with 11,202 entries) using MaxQuant (Tyanova et al., 2016). Carbamidomethyl Cysteine was set as a fixed modification. Oxidation of methionine and N-terminal acetylation were set as variable modifications. Tolerance for precursor ions was set to 4.5 ppm and 20 ppm for fragment ions. A maximum of two missed cleavages was allowed. MaxQuant was set to match in between runs and report LFQ. All other parameters were at the default setting. The proteinGroups.txt file generated by MaxQuant was further processed using Perseus. Reverse and possible contaminants were removed from the protein groups. Samples were separated into an experimental group consisting of the pull downs of isotype matched IgG (control) and a group consisting of the *Tb*TERT Immuno-Precipitation pull downs (3 IPs and 3 IgG controls). Protein groups were filtered to contain at least three quantifications in one experimental group. The remaining missing quantifications were imputed with random numbers from a normal distribution (width 0.3, shift = 1.8). A two-sided Student's t-test was performed across replicates between each experimental group.

MS bioinformatics analysis

The mass spectrometry proteomic data was analyzed by a range of approaches. The volcano plot was generated using GraphPad Prism software version 9.3.1. The STRING database was

used for classifying proteins based on functional categories and gene ontology (GO) terms. Protein-protein interaction network analysis was done using STRING version 11.5 (https://string-db. org/) and visualized by using the Cytoscape software version 3.9.1.

Structure-guided predictions

Proteins identified by mass spectrometry contained several hits that have very little primary sequence identity with proteins from other phyla, so their functional orthologs were not entirely evident from simple sequence homology. To identify whether structural homology exists between the local folds of these proteins and those reported in other organisms, we obtained predicted structure models of these *T. brucei* proteins from AlphaFold (Jumper et al., 2021) using their Uniprot IDs and then queried these 'PDB' entries using programs PDBeFold (Krissinel & Henrick, 2004) and DaliLite (Holm & Rosenstrom, 2010). The top scoring and only relevant hit with a DaliLite Z score cut-off of >2 is considered as biologically informative structural neighbor of the protein of interest.

Western blotting and SDS-PAGE analysis

All *Tb*TERT western blots were done using either an anti-FLAG antibody (1:500) or a custom anti-*Tb*TERT C terminus antibody (1: 500) unless otherwise indicated. Nucleolar protein 58 (NOP58) was detected using an anti-NOP58 antibody (Thermo Fisher Scientific, PA5-54321) diluted 1:500 and an anti-Rabbit HRP conjugated secondary antibody diluted to 1:10,000. To qualitatively check protein levels, 4 µL of IP eluate was separated on a 4%–12% Novex Tris-glycine gel and stained with Coomassie Brilliant Blue R-250 Dye (Thermo Scientific, 20,278)

for 30 min. The gel was then destained until bands were visible in destain solution (40% MeOH, 10% acetic acid).

TbTR detection and telomerase activity assay

*Tb*TERT IP was performed as described in the methods. To detect the presence of *Tb*TR in the IPed complex, total RNA was isolated from the protein G magnetic beads using the TRIzol reagent (Thermo Fisher Scientific, 15596026) following the manufacturers protocol. 100 ng of isolated RNA was then used for cDNA synthesis utilizing the SuperScript II reverse transcriptase (Thermo Fisher Scientific, 18064022) following the manufacturers protocol. The generated cDNA was then used for qRT-PCR analysis using *Tb*TR specific primers (Fwd: CTGTGG AAATTTGTCGTAAGTG, Rev: AGTAGGGTTAGGGATCGT ATAG).

To determine the activity of the Immunopurified *T. brucei* telomerase complex, a modified version of the exponential isothermal amplification of telomere repeat (EXPIATR) assay was performed (Dey et al., 2021; Tian & Weizmann, 2013) Briefly, A master mix was prepared on ice consisting of Nicking Telomerase Substrate (NTS, GTGCGTGAGAGCTCTTCCAATCCGTCGAGC AGAGTT), Nicking Probe (NP, AGCAGGAAGCGCTCTTCCTGC TCCCTAACCCTAACCC), 1X EXPIATR buffer (30 mM Tris-HCl, pH 8.3, 1.5 mM MgCl2, 100 mM KCl, 1 mM EGTA, 0.05% v/v Tween20), 200 µM dNTPs, Bst 2.0 Warm start DNA polymerase (0.96 units) and Nt. BspQ1 NEase (5 units). 17 µL of the master mix was aliquoted to PCR tubes containing, 3 µL of anti-FLAG bead bound *T. brucei* telomerase, RNase A treated or heat-inactivated telomerase RNP bound beads, telomerase positive control (TPC8, GTGCGTGAGAGCTCTTCCAATCCGTCGAGCAGAGTTAGG GTTAGGGTTAGGGTTAGGGTTAGGGTTAGGGTTAGGGTT AGGG) (0.5 µM) and blank

beads as a negative control. Telomerase activity was initiated by initial incubation of tubes at 28° C for 45 min for Nicking telomerase substrate (NTS) extension followed by amplification of resultant telomerase products at 55° C for 30 min. The amplified products were then analyzed on 12% Native PAGE gel by loading 10 μL of the reaction mixture.

2.3 Results

Affinity-purification mass spectrometry (AP-MS) of BF T. brucei telomerase reverse transcriptase

Characterizing the global interactors of a protein of interest can be done through affinity-purification mass spectrometry (AP-MS). Identifying the interactome of a protein is key in understanding its function in the cell and how it is regulated. To identify the global protein interactors of *T. brucei* telomerase, we utilized AP-MS to identify the global interactome of *Tb*TERT at the BF stage. We first immunopurified (IP) *Tb*TERT using a custom anti-*Tb*TERT antibody along with its associated proteins and performed LC-MS/MS (Fig. 5A). For immuno-affinity purification, 500 ul of lysate containing 1 mg of total protein was used per IP sample. *Tb*TERT was pulled down from the lysate using a custom anti-C terminus *Tb*TERT antibody (Dey et al., 2021). In addition to verifying the specificity of the custom antibody for binding to *Tb*TERT, the presence of some non-specific cross-reactive bands were also observed. The presence of the immunopurified *Tb*TERT was confirmed using western blotting and SDS-PAGE analysis (Fig. 5B–D). Immunoblot analysis (anti-FLAG antibody) of the IP fractions from *Tb*TERT-F2H cells showed that *Tb*TERT was enriched in the pulldown products from anti-*Tb*TERT C terminus antibody IPs but not from control groups. The anti-*Tb*TERT C-terminus antibody IP samples were then subjected to SDS-PAGE and in-gel protease digestion, followed by mass spectrometry as described in ‘Materials and Methods’. To further validate the presence of telomerase components in the IP, RNA was extracted from IP beads and subjected to qRT-PCR analysis to confirm the presence of the telomerase RNA in the complex (Figure 5E). To determine if the immunopurified telomerase complex was catalytically active, we performed a telomerase activity assay (EXPIATR) using the IPed complex (Figure 5F). The result confirmed

that the immunopurified *T. brucei* telomerase complex was catalytically active. To independently validate our proteomic screen, another set of affinity enrichment of *Tb*TERT protein using an anti-FLAG antibody was performed in duplicates in *Tb*TERT-F2H cells (two biological replicates) and screened for known *Tb*TERT interactors. Both the *Tb*TERT IP-MS and *Tb*TERT FLAG pulldown MS data were compared. Since *Tb*TERT and several other proteins that were previously linked to telomerase were identified in both FLAG and C-terminus IP mass spec data sets (Fig. 6; Supplementary Table S1**)** it was apparent that the ribonucleoprotein complex identified by this approach is biologically relevant to telomerase function.

Proteomic analysis of BF T. brucei Telomerase Reverse Transcriptase (TbTERT)

We identified 1,056 proteins with 2 or more peptides. After stringent filtering of this dataset for those proteins highly enriched (Log2(fold change) > 1.9) in the IP vs. control (Supplementary Table S1), 66 high-confidence proteins remained. To study the interactome of *Tb*TERT, the relative abundance (log2(fold change)) and statistical significance -log10(P-value) of the proteins from the IP samples and controls were calculated (3 IP samples and 3 IgG controls samples) (Fig. 6A). This resulted in the enrichment of 56 proteins for the anti-*Tb*TERT IP samples (Supplementary Table S2). The protein samples that were significantly enriched in the IP samples versus the controls (Student's t-test, -log10(P-value) > 1.3) included both nuclear and mitochondrial proteins that have previously been shown to interact with TERT or play a role in telomere maintenance, such as *T. brucei* telomerase reverse transcriptase (*Tb*TERT, Tb927.11.10190), yeast telomerase cell cycle turnover-related (anaphase promoting complex) proteins, CDC16 (Tb927.6.2150) and CDC27 (Tb927.10.10330) homologs (Ferguson et al., 2013; Sealey et al., 2011), mitochondrial stress-response protein, human HSP60 homolog

(Tb927.11.15040) which is known to accumulate with hTERT in the same fractions of human mitochondria (Sharma et al., 2012), Splicing factor 3B subunit 1 (SF3B1) homolog (Tb927.11.11850) involved in various cellular functions including DNA damage response (te Raa et al., 2015) and telomere maintenance (Wang et al., 2016), damage specific DNA binding protein 1 (DDB1) homolog (Tb927.6.5110), involved in ubiquitin-mediated TERT protein degradation (H. Y. Jung et al., 2013), and several other proteins involved in telomerase and telomere metabolism (selected proteins shown in Fig. 6A; Table 1).

To highlight the connectivity of candidate *Tb*TERT interactors, we used the STRING database and Cytoscape to generate a functional protein-protein interaction network of *Tb*TERT (Fig. 6B; Supplementary Figure S1). To further determine the functions of proteins in the network, STRING GO analysis was done, and proteins were grouped by biological process, and cellular component (Fig. 7A, B). The terms for biological process that were enriched included, telomere maintenance by telomerase, cell cycle control, DNA repair, and response to stress. Enriched cellular component terms included box C/D snoRNP complex, DNA replication factor C, anaphase-promoting complex, and cullin-RING ubiquitin ligase complex. Notably, proteins that are important for telomerase RNA biogenesis, processing and trafficking were significantly enriched in these GO terms.

An independent set of IP-MS using an anti-FLAG antibody to IP *Tb*TERT also validated many of the proteins identified in the mass spec run described above from the anti-C terminus *Tb*TERT IP because these proteins were identified with both IP approaches. A false discovery rate (FDR) of 1% was used as cut off for this data (Supplementary Table S3).

Known and novel interactors are part of the active telomerase RNP in T. brucei

Homologs of telomerase-associated proteins which are known regulators of telomerase functions were found to be part of the IP telomerase complex in *T. brucei*. Typically, three types of known telomerase-associated proteins were reported to co-purify with TERT. The foremost of the three are the telomerase RNA-binding proteins that are involved in TR biogenesis, trafficking and TR-TERT assembly. These include, for example, dyskerin in vertebrates (Mitchell & Collins, 2000; Mochizuki et al., 2004), Sm proteins in yeasts (Tang et al., 2012), and La-motif proteins, such as p65, in ciliates (Singh et al., 2012). Interestingly, dyskerin binding H/ACA domain of human TR is replaced by a novel C/D box domain in *T. brucei* (Gupta et al., 2013). Several unique C/D box snoRNA binding proteins (snoRNPs) were identified in our *Tb*TERT immunopurified complex which are described in the next section. In addition, a *T. brucei* La protein, Tb927.10.2370, which shows 24% amino acid sequence identity and a Z-score of 8.6 with *Tetrahymena thermophila*, TR binding protein p65 was also identified in the IP-MS. Telomerase RNP assembly also requires molecular chaperones, such as AAA+ family of ATPases, known as Pontin and Reptin, which can directly interact with TERT and play critical roles in telomerase RNP accumulation (Venteicher et al., 2008). Both the Pontin (Tb927.4.1270) and Reptin (Tb927.4.2000) homologs, annotated as RuvB-like DNA helicases in the *T. brucei* genome database, were also identified by this *Tb*TERT AP-MS analysis. Additionally, another AAA+ ATPase protein, a yeast CDC48 homolog, Tb927.10.5770, was also identified. CDC48, which was previously identified in a molecular complex that recognized and bound ubiquitinated proteins (Schuberth et al., 2004), was also found to be associated with yeast telomerase as a novel regulator of telomere length homeostasis. Notably, TERT turnover is dependent on ubiquitin-proteasome mediated degradation process (Jung et al., 2013) and therefore proteins that are important for ubiquitination were previously identified in the telomerase complexes, such as

several isoforms of E3 ubiquitin ligases (Lin et al., 2015). Interestingly, several ubiquitin-family proteins were also identified in the IP-MS data including ubiquitin ligases, although the roles of these proteins in *T. brucei* telomerase biology remains uncertain until the ubiquitination status of *Tb*TERT is determined.

Mammalian studies have identified chaperone proteins p23 and HSP90 as two important proteins that are physically and functionally associated with telomerase activity (Holt et al., 1999). The proteomic mapping also identified a mammalian HSP90 homolog, Tb927.3.3580, with enrichment of several unique peptides in *Tb*TERT IP samples identified by MS. Poly(A)-specific ribonuclease (PARN) is a 3′-exoribonuclease that is known to play important role in the maturation of telomerase RNA (Moon et al., 2015). A *T. brucei* homolog of PARN, Tb927.9.13510 was identified in this proteomic mapping data that may relate with the fact that *T. brucei* telomerase RNA is a Pol II transcript (Sandhu et al., 2013) that may require PARN processing for maturation. All these known telomerase homologs of *T. brucei* are listed in Supplementary Table S1. In terms of proteomic identification, it should be noted that several of the above proteins were identified in the range of low scoring functions or higher FDR %, however, these proteins are identified in all four of the biological replicates analyzed by AP-MS and therefore could be biologically relevant. Importantly, all the above proteins identified were part of the IP sample that was able to extend *T. brucei* telomeric repeats using synthetic TTAGGG as substrates in activity assays (Figure 5F), indicating that the proteins in this IP are potentially part of an active telomerase complex.

The unique C/D box domain in T. brucei telomerase RNA is bound by snoRNPs

In contrast to hTR, the telomerase RNA in *T. brucei* contains a unique C/D snoRNA-like domain (Fig. 8A bottom). Core C/D box RNPs, like NOP58, have previously been shown to interact with *Tb*TR (Gupta et al., 2013). NOP58 is a 57 KDa protein that contains a coiled-coil (CC) domain and a NOP domain (Fig. 8A top). NOP58 is highly conserved across eukaryotes and plays important roles in ribosomal RNA (rRNA) processing (Barth et al., 2008). In our AP-MS analysis of *Tb*TERT, we identified three core C/D box binding proteins: NOP58, NOP56, and Fibrillarin (NOP1) (Table 2; Supplementary Table S3). To validate the interaction with NOP58, we performed a co-immunoprecipitation (Co-IP) assay of *Tb*TERT and detected *Tb*TERT and NOP58 through western blotting (Fig. 8B top). For further confirmation of this interaction, we performed Co-IPs of *Tb*TERT in both WT and ΔC/D box mutant cell lines. In the WT cells, NOP58 is present in the IP product, while in the ΔC/D mutant cells, the interaction with NOP58 is greatly diminished (Fig. 8B bottom). This data supports the fact that the C/D box motif is important for the interaction between *Tb*TR and NOP58.

2.4 Discussion

Eukaryotic microbes, such as *T. brucei*, rely on constitutive telomerase activity to sustain their proliferation in their hosts and to maintain the integrity of their sub-telomeric virulence genes. Studying these interacting partners of telomerase in *T. brucei* is necessary to characterize the mechanism of telomerase mediated telomere maintenance in these parasites. Like any other RNA component of telomerase, *T. brucei* telomerase RNA in the holoenzyme acts as a structural scaffold that accessory proteins can bind to (Dey and Chakrabarti, 2018). Interacting proteins of telomerase in *T. brucei* have not been extensively studied. We have utilized a mass spectrometry approach to identify and characterize endogenous interactions of *Tb*TERT in BF *T. brucei* cells. However, characterization of dynamic RNA-protein interactions like the one in telomerase

complex comes with a challenge that several of these interaction partners could be only transiently bound and therefore may not represent the complex interactions in its entirety. Nonetheless, this affinity purification based proteomic characterization of *T. brucei* telomerase RNP complex provides a global view of the cellular protein interactome landscape that can be used for in-depth functional characterization of telomerase complex proteins in parasites.

Some potential limitations of this study are the use of affinity purification methods. These methods are good at isolating strong interactions of our bait protein *Tb*TERT, but as mentioned above, weaker, or more transient interactions may be missed by this analysis. Also, proteins of low abundance, such as TERT, could be difficult to enrich in affinity purified complexes even by targeted approaches like RNA-targeted APEX based proteomic approach recently employed for human telomerase (Han et al., 2020). For that reason, it is possible that several *Tb*TR and *Tb*TERT associated proteins that are identified in this proteomic screen showed low level of enrichment in the IP complex, as evident from MS. Since IP experiments using MS provide a sensitive and accurate way of characterizing protein complexes, the quality of antibody may also play a role in isolating and analyzing specific interactions. The custom anti-*Tb*TERT polyclonal antibody used in the IP experiments was cross-reactive to other proteins (data not shown), however, the binding specificity to the endogenous bait protein *Tb*TERT was successfully confirmed using Co-IP and Western blot as *Tb*TERT was detected as a single, discrete band. Additionally, detection of the telomerase-associated proteins in all biological replicates added confidence to the current approach.

Our proteomics experiments also identified proteins that have no known relationship with telomerase and therefore these hits could be false positives or newly discovered interactors of *Tb*TERT. For example, an RNA cytidine acetyltransferase, NAT10 homolog (Tb927.5.2530)

was found enriched in all proteomic datasets. NAT10 was previously shown to have predominantly nucleolar localization, association with human telomerase, and is primarily involved in telomerase RNA biogenesis (Fu & Collins, 2007). One more example is the putative NOT1 deadenylase (Tb927.10.1510), part of the CCR4-NOT deadenylase complex, which plays important regulatory roles both at the transcriptional and post-transcriptional levels, such as heterochromatic repression of sub-telomeric genes in fission yeast (Cotobal et al., 2015) and rapid deadenylation of m6Acontaining RNAs by the CCR4–NOT deadenylase complex in mammalian cells (Du et al., 2016). Given that a majority of expressed virulence genes (VSGs) in *T. brucei* are sub-telomeric (Saha et al., 2020) and human telomerase RNAs are known to contain m6A signatures (Han et al., 2020), the role of Tb927.10.1510 remains unexplored but relevant to *T. brucei* telomere biology.

In our proteomics screen, several mitochondrial proteins were highly enriched, including *Tb*UMSBP2, which has been shown to associate with telomeres in *T. brucei* (Klebanov-Akopyan et al., 2018). This protein's canonical function is the replication and segregation of *T. brucei's* mitochondrial DNA, but it has been shown to also play a role in chromosome end protection in *T. brucei* (Klebanov-Akopyan et al., 2018). Significantly enriched GO terms from the analysis of the *Tb*TERT interactome included telomere maintenance via telomerase, cell cycle control, and chaperone binding. Similar terms and protein interactors have been previously observed for Saccharomyces cerevisiae telomerase (Lin et al., 2015). Telomere maintenance via telomerase is consistent with *Tb*TERT's known role in extending telomeres (Dreesen & Li, 2005). Enrichment of proteins involved in cell cycle control highlight potential factors involved in the cell cycle specific regulation of *Tb*TERT. Specifically, APC3 and CDC16 were significantly enriched in the *Tb*TERT interactome. APC3 and CDC16 are core components of the anaphase-promoting

complex (APC), which is a 1.5 MDa ubiquitin ligase complex that regulates sister-chromatid separation and the cells exit from mitosis (Peters, 2006). In S. cerevisiae, the APC has been shown to degrade the telomerase recruitment subunit, Est1p to regulate telomere maintenance (Ferguson et al., 2013). Whether an analogous mechanism exists in *T. brucei* remains to be explored.

Chaperone proteins such as DnaJ, which is a major co-chaperone for HSP70 and HSP60 were also found to be significantly enriched in the *Tb*TERT interactome. Both DnaJ and HSP60 have previously been found to associate with human telomeres (Nittis et al., 2010). HSP60 is a predominately mitochondrial chaperone, where it works to maintain protein homeostasis (Bayisotto et al., 2020). In human cells, TERT has been previously reported to localize to the mitochondria and guard cells against oxidative stress (Ahmed et al., 2008). Human TERT has also been shown to associate with HSP60 and act independently of the TR in the mitochondria (Sharma et al., 2012). *Tb*TERT's association with HSP60 suggests a pool of *T. brucei* telomerase may also be localized in the mitochondrion.

In addition to proteins involved in cell cycle control and chaperones, core C/D snoRNP proteins, NOP58, NOP56, and Fibrillarin (NOP1) were also identified in the *Tb*TERT interactome. Our co-IP western blot data validates the interaction of NOP58 with the *T. brucei* telomerase complex. NOP58 interacts with NOP56 and NOP1 to form a subcomplex, which participates in rRNA processing (Barth et al., 2008). Core C/D box binding proteins, like NOP58, have been previously shown to interact with the TbTR (Gupta et al., 2013). Our study supports these findings and shows that NOP58 interacts with the C/D box motif in the *Tb*TR. The C/D box motif in *Tb*TR is unique and lacking in higher eukaryotes. The TR in Leishmania also contains a C/D box motif (Vasconcelos et al., 2014). The conservation of the C/D box motif

in the TR of these parasites could indicate a novel mechanism for telomerase biogenesis and processing, mediated by C/D box binding proteins, in these kinetoplastid parasites.

The work described here provides the first analysis of the *Tb*TERT interactome. We have identified previously known and novel interactors of *Tb*TERT. We were able to confirm NOP58's interaction with the *T. brucei* telomerase complex, which supports earlier studies (Gupta el al., 2013). Taken together our study lays the foundation for future studies into the mechanism of telomerase mediated telomere maintenance in *T. brucei*. Future improvements are needed to develop a telomerase RNA -tagged proteomic mapping approach in *T. brucei* to validate endogenous interactions identified by this method and detect new RNA-specific interactions. Future studies should also benefit from investigating interactomes from other *T. brucei* developmental stages since it appears from our recent study that *T. brucei* telomerase function is developmentally regulated (Dey et al., 2021). Therefore, characterizing stage-specific interactomes can provide novel insights into regulatory mechanisms that can affect rate of proliferation and telomerase activity in *T. brucei*.

2.5 Figures

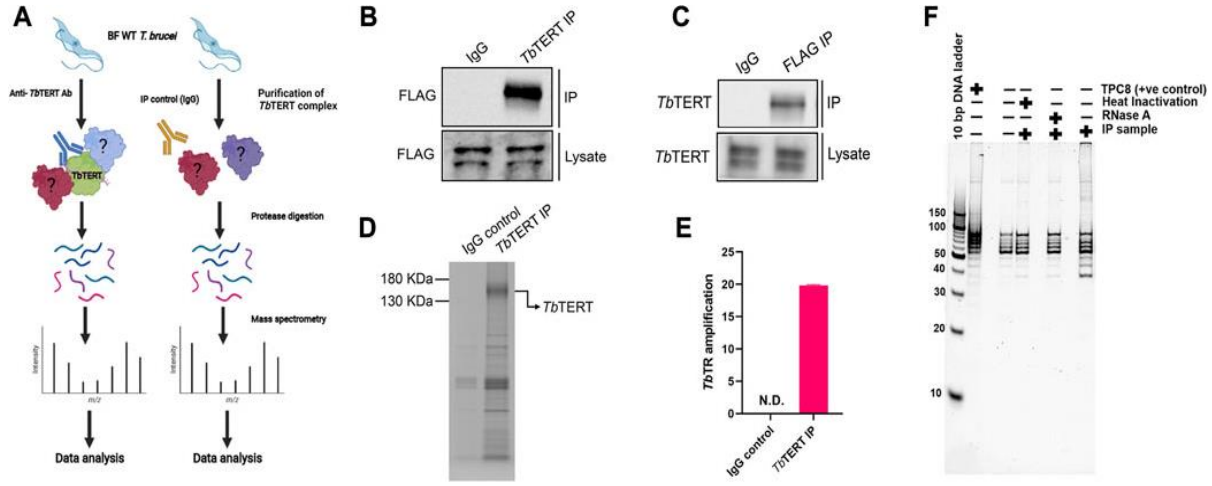

Figure 5. Affinity-purification mass spectrometry of bloodstream form *T. brucei* telomerase reverse transcriptase. (A) Experimental workflow for proteomic analysis. BF *T. brucei* cells expressing a FLAG tagged version of *Tb*TERT were grown and *Tb*TERT complexes were purified using a custom anti-*Tb*TERT C terminus antibody. An IgG isotype antibody was used as a control. Purified *Tb*TERT complexes were then digested with trypsin. These peptides were then analyzed by LC-MS/MS. (B) Western blot confirming the presence of immunopurified *Tb*TERT. IP samples were obtained and run on SDS-PAGE gels and immunoblotted with anti-FLAG antibody to detect *Tb*TERT. (C) Western blot confirming the presence of *Tb*TERT. IP samples were obtained and run on SDS-PAGE gels and immunoblotted with an anti-*Tb*TERT C terminus antibody to detect *Tb*TERT. (D) SDS-PAGE analysis of immunopurified *Tb*TERT. A small aliquot was also resolved on SDS-PAGE and stained with Coomassie stain to qualitatively check *Tb*TERT protein levels. (E) RT-qPCR detection of *Tb*TR from Immunopurified *Tb*TERT complexes. (F) Telomerase activity of the bead-bound telomerase enzyme was analyzed by telomerase primer extension assay.

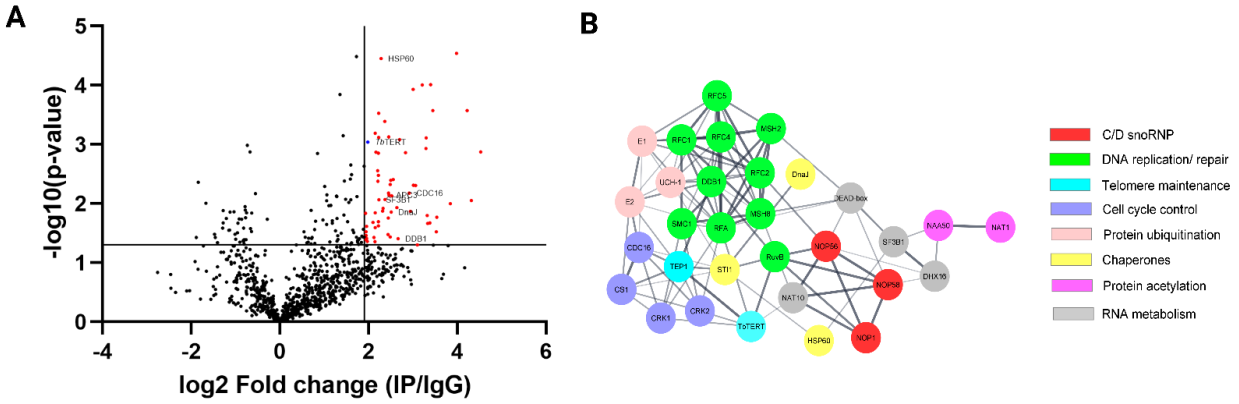

Figure 6. Proteomic analysis of BF *T. brucei* telomerase reverse transcriptase.
(A) Volcano plot was performed with an *x*-axis representing the difference in logarithmic protein intensities between the *Tb*TERT immunoprecipitation elution and the isotype matched IgG control (Elution and Control experimental groups). The *y*-axis is the negative log of the two-sided Student's t-test. The volcano plot serves as a visual representation of the protein groups that are significantly enriched between the elution and control groups. These enriched groups contain the bait protein *Tb*TERT and several candidates interacting with a *p*-value ≤ 0.05. (B) Protein-protein interaction network of relevant *Tb*TERT hits identified by MS. Network was generated using the STRING database and visualized using Cytoscape. Colors of nodes represent the protein's biological function. The thickness of the lines denotes the strength of the interaction (confidence PPI, threshold: 0.4, medium confidence).

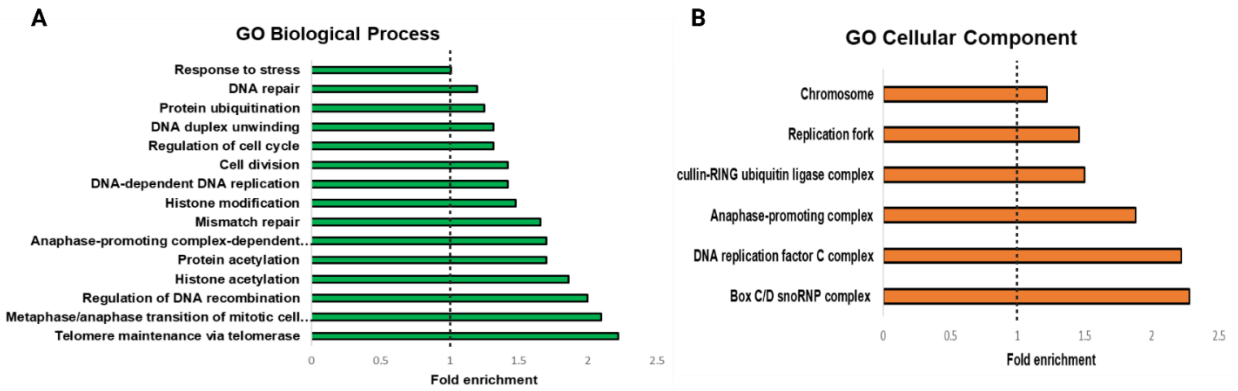

Figure 7. GO analysis of T. brucei TERT interactome. STRING GO analysis (A) Enrichment by Biological process. The top 15 enriched GO terms are shown. (B) Enrichment by Cellular component. The top 9 enriched GO terms are shown.

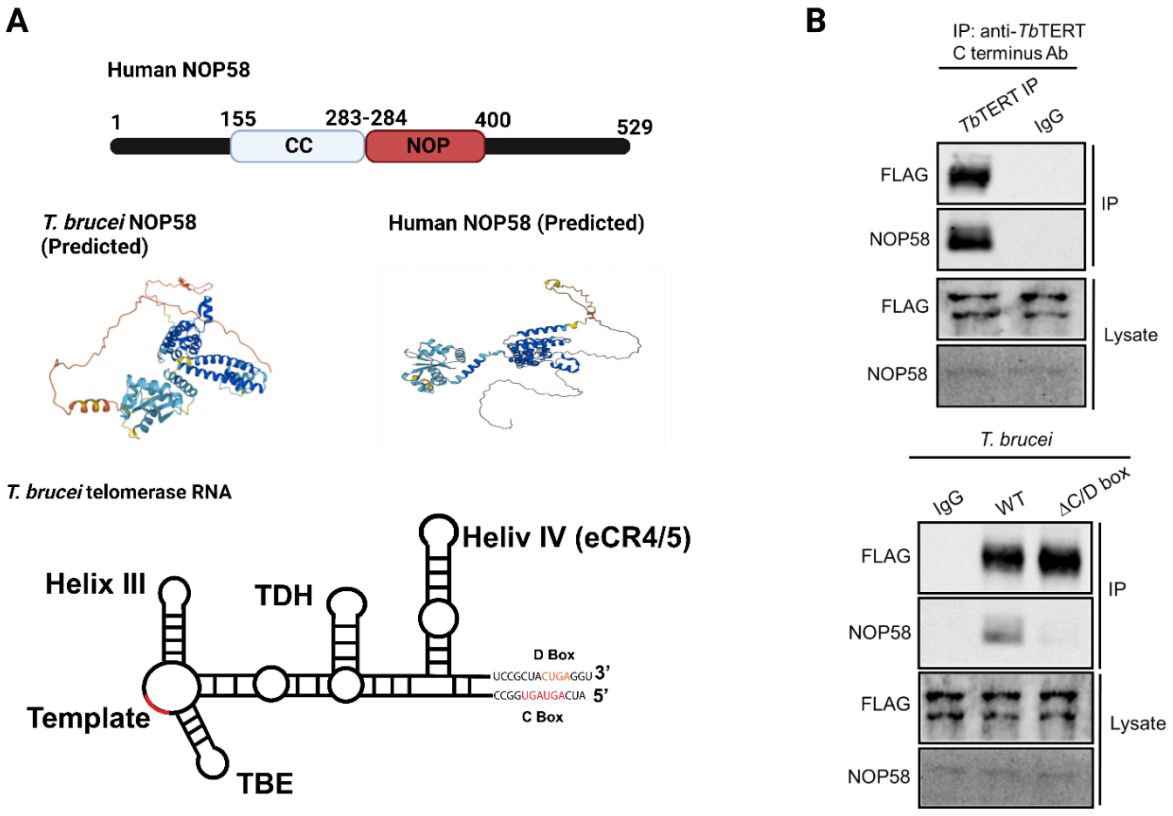

Figure 8. NOP58 interacts with the *T. brucei* telomerase complex. (A) Domain structure of human NOP58. Predicted secondary structure models for *T. brucei* and human NOP58 obtained from AlphaFold (Jumper et al., 2021) Predicted protein structures are shown in the same orientation. Dark blue represents a very high model confidence (pLDDT >90), light blue confident (90 > pLDDT >70), yellow low confidence (70 > pLDDT >50), orange very low confidence (pLDDT <50). Secondary structure model of *T. brucei* telomerase RNA. The C/D box binding motif is highlighted. (B), top Co-IP assay using WT *T. brucei* cell lysate. IP antibody: anti-*Tb*TERT C terminus; Western blot antibodies: anti-FLAG and anti-NOP58. (B), bottom Co-IP using both WT and ΔC/D box mutant cells. IP antibody: anti-*Tb*TERT C terminus; western blot antibodies: anti-FLAG and anti-NOP58.

Table 1. Significantly enriched proteins identified in *Tb*TERT complex.

Protein	Accession number	Spectral counts	Unique peptides (UniProtKB)
*Tb*TERT	Q383RO	10	5
HSP60	Q381Tl	6	5
DnaJ	Q38C15	19	5
APC3	Q389U4	21	6
CDC16	Q584Ul	30	12
SF3Bl	Q382Z6	26	14
DDBl	Q586I3	21	13

Table 2. Core C/D snoRNPs identified in *Tb*TERT complex.

Protein	Accession number (UniProtKB)	Spectral counts	Unique peptides
NOP58	Q38F23	25	12
NOP56	Q580Z5	24	10
Fibrillarin/NOPl	Q388EO	8	3

Supplementary table 3 *T. brucei* TERT interacting partners – known homologs

Gene/Protein	Gene ID	UniProt ID	Unique Peptides	*DaliLite Z-score	minusLog10(P-value) /log2 Fold Change	
					TbTERT Ab IP-MS	FLAG IP-MS
Heat shock protein 90 (**HSP90**), putative	Tb927.3.3580	Q57W94	35	31.0	1.52/ -0.64	.12/ -0.72
AAA family ATPase, **CDC48** homolog of *S.cerevisiae*)	Tb927.10.5770	Q38B27	33	49.4	0.226/ 0.113	0.14/ -0.61
RuvB-like DNA helicase, (**PONTIN**) putative	Tb927.4.1270	Q581V4	17	41.9	0.136/ -0.09	0.73/ -2.3
RuvB-like DNA helicase, (**REPTIN**) putative	Tb927.4.2000	Q583J3	13	39.4	1.58/ -0.82	0.02/ -0.04
Nucleolar protein 58 (**NOP58**), putative	Tb927.9.5320	Q38F23	12	26	0.27/ 0.75	1.08/ 2.25
Poly(A)-specific ribonuclease **PARN**, putative	Tb927.9.13510	Q38D76	11	32.8	0.87/ 1.3	0.65/ 2.2
Replication factor A protein 1	Tb927.11.9130	Q384B5	10	20.8	0.11/ -0.18	0.34/ 0.56
Nucleolar protein 56 (**NOP56**), putative	Tb927.8.3750	Q580Z5	10	27.2	0.4/ -0.15	0.8/ 1.90
Telomerase Reverse Transcriptase (***Tb*TERT**)	Tb927.11.10190	Q383R0	5	22.9	3.0/ 1.98	0.38/ 0.49
La protein (**p65**) homolog, putative	Tb927.10.2370	Q38C07	3	8.6	0.19/ -0.63	0.09/ -0.49
Fibrillarin, putative	Tb927.10.14630	Q388C9	3	33.5	0.26/ 0.27	0.78/ 1.97

*'Significant similarities' have a Z-score above 2; they usually correspond to similar folds when searched against entire PDB matches.

Figure 9. Table of interacting proteins identified in BF *Tb*TERT. S1 and S2 tables can be found in the supplemental of Davis et al., 2023.

CHAPTER 3: PROTEOMIC COMPOSITION OF TELOMERASE IN THE PROCYCLIC FORM OF *TRYPANOSOMA BRUCEI* AND POST-TRANSLATIONAL MODIFICAITON PROFILE OF TERT

3.1 Introduction

Chromosomes in eukaryotic organisms are linear. Because of this, they contain specialized structures at their ends termed telomeres. Telomeres are composed of both double-stranded and single-stranded DNA regions and are bound by telomeric binding proteins (de Lange, 2018). Telomeres pose a unique challenge to cells as endogenous DNA polymerases are unable to fully replicate the DNA all the way to the end. This "end-replication problem" leads to the progressive loss of DNA after every cell division and telomeric shortening. The end-replication problem is solved by the actions of the enzyme telomerase. Telomerase is an RNA-protein enzyme that consists of two main components: the telomerase reverse transcriptase (TERT) protein that catalyzes telomeric extension, and the telomerase RNA (TR) that provides the template for telomere synthesis (Greider & Blackburn, 1985, 1989). The actions of telomerase help cells preserve their telomere length and maintain genome integrity.

A key mechanism of protein regulation inside cells is the addition of post-translational modifications (PTMs) onto proteins. These modifications in cells can range from diverse chemical groups to whole proteins. These modifications help fine tune protein regulation inside the cell across a variety of molecular pathways. The telomerase protein has also been shown to be regulated by PTMs. PTMs of TERT protein have been well studied in human TERT (hTERT). The two most well studied modifications with regards to hTERT regulation are phosphorylation and ubiquitination. Phosphorylation of hTERT has been shown to regulate the enzymes catalytic activity as well as its cellular localization (Kang et al., 1999; Kharbanda et al., 2000). Some of the writer enzymes of hTERT Phosphorylation have also been identified and

studied. The AKT kinase has been previously shown to phosphorylate hTERT at serine 227 to direct its nuclear localization (Chung et al., 2012). Another phosphorylation site that has been identified and studied in hTERT is tyrosine 707. This residue has been shown to be phosphorylated by the SRC kinase under oxidative stress to promote hTERT translocation from the nucleus to the cytoplasm (Haendeler et al., 2003). Ubiquitination is another modification on hTERT that has been identified and studied. Several writers of hTERT ubiquitination have also been identified. The E3 ubiquitin ligase, Makorin RING finger protein 1 (MKRN1) has been shown to ubiquitinate TERT, likely to mark hTERT for degradation through the ubiquitin proteasomal system (Kim et al., 2005). More recent studies have also demonstrated that ubiquitination controls hTERT protein levels in a cell cycle dependent manner (H.-Y. Jung et al., 2013). During G2/M phase, the Dyrk2 associated EDD-DDB1-VprBP E3 ligase complex catalyzes the addition of poly ubiquitin chains onto hTERT. hTERT then undergoes degradation and telomerase activity is inhibited (H.-Y. Jung et al., 2013).

Trypanosoma brucei (*T. brucei*) is a protozoan parasite that causes African sleeping sickness in humans. *T. brucei* has a two-host life cycle where it will shuttle between an insect (*Glossina* spp.) and a human host. During this time the parasite will transition between distinct developmental stages. The procyclic form (PF) found in the insect's mid-gut and the bloodstream form (BF) found in the human bloodstream. *T. brucei*, like many eukaryotic pathogens, relies on constant telomerase activity to sustain the high levels of cell division necessary to establish a successful infection in its human host. PTMs and protein-protein and RNA-protein interactions are just a few of the modes of regulation employed by *T. brucei* to regulate protein function. Identifying interacting proteins of a protein of interest can provide novel insight into that proteins

function and regulation. The interactome of BF *Tb*TERT has been reported (Davis et al., 2023), but the PF *Tb*TERT interactome remains to be identified.

PTMs play a key role in regulating a variety of molecular pathways inside cells including telomerase regulation. PTMs have been identified in *T. brucei* previously and have been found to play important regulatory roles (Zhang et al., 2021; Zhang et al., 2020). These modifications in *T. brucei* have been found on protein belonging to a variety of molecular pathways including, RNA-binding proteins, metabolic proteins and histones (Zhang et al., 2020). This suggests in *T. brucei*, like other eukaryotes, PTMs play a key role in regulating a variety of cellular processes. PTMs on telomerase have not been extensively identified across eukaryotes and there have been no PTMs identified on *T. brucei* TERT (*Tb*TERT). In this work, we have utilized a mass spectrometry-based approach to identify the global interactome of PF *Tb*TERT and novel PTM sites on *Tb*TERT in an unbiased manner. One major advantage was to use a cell line which contains GFP-tagged TERT under the control of a doxycycline inducible promotor. This allowed us to induce the overexpression of *Tb*TERT-GFP by addition of doxycycline. This combined with using an anti-GFP antibody, allowed us to greatly increase the amount of *Tb*TERT protein we can pull down from our IP samples. In our global interactome analysis of PF *Tb*TERT we identified similar core telomerase interacting proteins that were previously identified in the BF *Tb*TERT interactome (Davis et al., 2023). This conservation highlights the essentiality of core telomerase interacting proteins across *T. brucei's* life cycle. We have also employed mass spectrometry to map PTMs on PF *Tb*TERT and were able to identify 30 novel modified sites throughout the *Tb*TERT protein. We were also able to identify a novel N-terminal acetylation site in *Tb*TERT that has not been identified in any other eukaryote. Our study provides the first reported interactome of telomerase from *T. brucei* insect stages and the first detailed list of PTMs

on *Tb*TERT and lays the foundation for future mechanistic studies to probe the biological role of these modifications in *Tb*TERT regulation.

3.2 Materials and Methods

Culture of procyclic form (PF) T. brucei cells

T. brucei Lister strain 427 was used throughout this study. All PF cells were grown in SDM-79 media supplemented with 10% heat inactivated Fetal Bovine Serum (FBS) at 27°C. PF T. brucei cells expressing a TERT-GFP fusion protein were grown in media containing 20 µg/mL of G418, 40 µg/mL of Hygromycin, 2.5 µg/mL of phleomycin and 1 µg/mL of doxycycline was used to induce overexpression of the TERT-GFP fusion protein.

Immunopurification of T. brucei telomerase complexes

Immunopurification of telomerase complexes from PF *Tb*TERT-GFP cells was done by collecting 5-6x10^8 cells/ 60 mL by centrifugation at 800XG for 10 minutes. Following centrifugation, cells were lysed by homogenization in 300 µL of 1X immunopurified (IP) lysis buffer (25 mM Tris-HCl pH 7.5, 150 mM KCl, 1 mM EDTA, 10 mM MgCl2, 0.5% IGEPAL CA630, 1X protease cocktail inhibitor, and 20 units of Ribolock RNase inhibitor, 1X sodium fluoride and 1X sodium orthovanadate). Lysate was then cleared of cell debris by centrifugation at 3000 RPM for 5 min at 4°C. Cleared lysates were then incubated with 2.4 µg/mL of anti-GFP antibody (Invitrogen, A-11122) overnight at 4 C on rotation. Following overnight incubation, the lysate-antibody mixture was further incubated with 50 µl of pre-washed protein-G Dynabeads (Invitrogen, 10003D) for two hours on rotation at 4 C. The beads were then washed twice in IP wash buffer (25 mM Tris-HCl pH 7.5, 150 Mm KCl, 1 mM EDTA, 10 Mm MgCl2, 1X protease inhibitor cocktail, 20 units of Ribolock RNase inhibitor, 1X sodium fluoride and 1X sodium orthovanadate) and once in 1X PBS. Beads were then resuspended in 50 µL of 1X PBS and stored in -80 C until further use.

Western blotting and SDS-PAGE analysis

Western blotting was carried out using 4–12% polyacrylamide Bis-Tris Glycine gels (Life Technologies) and the polyclonal antibody against *Tb*TERT C-term was used as a primary antibody with 1:500 dilution. Horseradish Peroxidase (HRP) conjugated anti-rabbit secondary antibodies (Abcam, ab6721) were used at 1:10000. Detection was carried out using Pierce ECL Plus Chemiluminescence substrate kit (Thermo-Fisher Scientific, 32106). To qualitatively check protein levels, the IP eluate was separated on a 4%–12% Novex Tris-glycine gel and stained with Coomassie Brilliant Blue R-250 Dye for 30 min. The gel was then destained until bands were visible in destain solution (40% MeOH, 10% acetic acid).

MS sample preparation

On bead samples were submitted to the IUSM Center for proteome analysis where proteins were denatured in 8 M urea, 100 mM Tris-HCl, pH 8.5 and reduced with 5 mM tris(2-carboxyethyl) phosphine hydrochloride (TCEP, Sigma-Aldrich Cat No: C4706) for 30 minutes at room temperature. Samples were then alkylated with 10 mM chloroacetamide (CAA, Sigma Aldrich Cat No: C0267) for 30 min at room temperature in the dark, prior to dilution with 50 mM Tris.HCl, pH 8.5 to a final urea concentration of 2 M for Trypsin/Lys-C based overnight protein digestion at 37 ºC (0.5 µg protease, Mass Spectrometry grade, Promega Corporation, Cat No: V5072.).

Peptide purification and labeling

Digestions were acidified with trifluoroacetic acid (TFA, 0.5% v/v) and desalted on Pierce C18 spin columns (Thermo Fisher Cat No: 89870) with a wash of 0.5% TFA followed by elution in 70% acetonitrile 0.1% formic acid (FA).

Nano-LC-MS/MS

Mass spectrometry was performed utilizing an EASY-nLC 1200 HPLC system (SCR: 014993, Thermo Fisher Scientific) coupled to Exploris 480™ mass spectrometer with FAIMSpro interface (Thermo Fisher Scientific). 1/5th of each fraction was loaded onto a 25 cm IonOpticks-TS column (Ionopticks Aurora Ultimate TS 25cm) at 350 nL/min. The gradient was held at 5% B for 5 minutes (Mobile phases A: 0.1% formic acid (FA), water; B: 0.1% FA, 80% Acetonitrile (Thermo Fisher Scientific Cat No: LS122500)), then increased from 4-30%B over 98 minutes; 30-80% B over 10 mins; held at 80% for 2 minutes; and dropping from 80-4% B over the final 5 min. The mass spectrometer was operated in positive ion mode, default charge state of 2, advanced peak determination on, and lock mass of 445.12003. Three FAIMS CVs were utilized (-40 CV; -55 CV; -70CV) each with a cycle time of 1.3 s and with identical MS and MS2 parameters. Precursor scans (m/z 375-1500) were done with an orbitrap resolution of 120000, RF lens% 40, automatic maximum inject time, standard AGC target, minimum MS2 intensity threshold of 5e3, MIPS mode to peptide, including charges of 2 to 7 for fragmentation with 30 sec dynamic exclusion. MS2 scans were performed with a quadrupole isolation window of 1.6 m/z, 30% HCD CE, 15000 resolution, standard AGC target, automatic maximum IT, fixed first mass of 110 m/z.

Mass spectrometry Data Analysis

Resulting RAW files were analyzed in Proteome Discover™ 2.5 (Thermo Fisher Scientific) with a *T. brucei* reference proteome FASTA (downloaded from Uniprot 8658 entries) plus common contaminants (73 entries) (Orsburn, 2021). SEQUEST HT searches were conducted with a maximum number of 3 missed cleavages; precursor mass tolerance of 10 ppm, and a fragment mass tolerance of 0.02 Da. Static modifications used for the search were

carbamidomethylation on cysteine (C). Dynamic modifications included oxidation of methionine (M), and acetylation, methionine loss, or methionine loss plus acetylation on protein N-termini. Percolator False Discovery Rate was set to a strict peptide spectral match FDR setting of 0.01 and a relaxed setting of 0.05. In Raw data were also analyzed using Peaks X Pro studio (Bioinformatics solutions Inc) to identify more potential post translational modifications (Cracco et al., 2022; Tran et al., 2019). PEAKS database search was done against *T. brucei* reference proteome FASTA (downloaded from Uniprot 8658 entries) using parent mass error of 10.0 ppm, fragment mass error of 0.02, specific trypsin with [D][P] cleavage with carbamidomethyl (C) as static and oxidation (M), phosphorylation (STY), and N-term acetylation as variable modification with a maximum of 3 variable PTMs per peptide. This search was followed by PEAKS PTM searching for over 317 potential PTMs with FDR estimation enabled, de novo score threshold of 15% and peptide hit threshold of -logP=30. A Spider search for mutations was also performed. Data were filtered for a peptide FDR<1%.

MS bioinformatic data analysis

The proteomic data generated by mass spectrometry was analyzed using a variety of approaches. The STRING database was used for classifying proteins based on functional categories and gene ontology (GO) terms. Protein-protein interaction network analysis was done using STRING version 11.5 (https://string-db.org/) and visualized by using the Cytoscape software version 3.9.1.

3.3 Results

Affinity-purification mass spectrometry to determine proteomic composition of PF *Tb*TERT

Studying the interactors of a protein of interest can be a great way to gain novel insights into a protein's function and regulation. The interactome of *Tb*TERT has been reported in the BF stage of this parasite (Davis et al., 2023). Telomerase activity appears to be developmentally regulated in *T. brucei*. Previous work has shown differences in TR structure and telomerase activity between the two developmental stages (Dey et al., 2021). To determine if there are developmental differences in *Tb*TERT interactions, we have utilized an affinity-purification mass spectrometry-based approach to identify the global interactome of *Tb*TERT in the PF developmental stage of *T. brucei*. We first immunopurifed (IP) *Tb*TERT from PF *T. brucei* cells expressing a *Tb*TERT-GFP fusion protein under the control of a doxycycline inducible promoter. 1 µg/mL of doxycycline was added to the culture media prior to *Tb*TERT IP. This IP was done using an anti-GFP antibody to partially purify the *Tb*TERT and its associated proteins. The presence and abundance of the *Tb*TERT protein was confirmed by SDS-PAGE analysis and western blotting (Fig. 10). Western blotting analysis confirmed the presence of the *Tb*TERT-GFP protein in the IP elution's tested. The IP samples were then subjected to on-bead protease digestion followed by mass spectrometry as described in the "materials and methods".

Proteomics analysis of PF *T. brucei* telomerase reverse transcriptase

We identified approximately 1019 proteins in the PF *Tb*TERT interactome with 7 or more unique peptides. Stringent filtering of this list for proteins was based on, reproducibility (two out of three biological replicates), unique peptide number (< 7) known relevance to telomere maintenance and core proteins that were previously identified in the BF *Tb*TERT

interactome (Davis et al., 2023). To characterize the PF *Tb*TERT interactome in more detail, we used the STRING database and cytoscape to generate a protein-protein interaction network of PF *Tb*TERT (Fig. 11A). STRING GO analysis was then performed to assign functionality to the proteins identified in this interactome. Proteins were grouped by biological process and cellular component (Fig. 11B). The terms that were enriched for biological process included, response to stress, DNA repair, DNA replication and DNA metabolic process. Enriched cellular component terms included, DNA replication factor C complex, box C/D RNP complex, protein acetyltransferase complex and the chromosome.

Affinity-purification mass spectrometry to map *T. brucei* TERT PTMs

Mapping PTMs on a protein of interest can be done using affinity-purification mass spectrometry (AP-MS). MS has the added advantage of not only identifying what the PTM is, but also has the potential to identify the specific amino acid residues that are being modified. Identifying PTMs on a protein of interest is an important first step in understanding the potential roles PTMs play in regulating that protein's function. To map PTMs on *Tb*TERT, we have utilized an AP-MS approach to identify PTM sites on the *Tb*TERT protein in the PF developmental stage of this parasite. We did this by first performing an immunopurification (IP) of the *Tb*TERT protein from PF *T. brucei* cells expressing a fusion protein of *Tb*TERT and GFP. This was done using an anti-GFP antibody to partially purify the *Tb*TERT protein, which was then subjected to LC-MS/MS analysis. For immune-affinity purification, 500 µl of lysate was used per IP sample. The presence of the immunopurified *Tb*TERT was confirmed using SDS-PAGE analysis and western blotting (Fig. 10). Western blotting analysis (anti-*Tb*TERT antibody) of the IP elutions from PF *Tb*TERT-GFP cells, revealed that the *Tb*TERT protein was

successfully enriched in the elution's tested (Fig. 10B). IP samples used for analysis were kept bound to the magnetic beads used following IP and subjected to on-bead digestion followed by LC-MS/MS analysis outlined in the "materials and methods" section.

From our MS analysis, we have obtained ≈62% *Tb*TERT sequence coverage from our PF *Tb*TERT-GFP IP samples. Our experiments were done in biological triplicate (n= 3) with 52-56 *Tb*TERT peptides identified in a typical experiment. As a result, we were able to identify 30 novel modified sites on *Tb*TER. The identified modifications included: N-terminal acetylation, 2-amino-3-oxo-butanoic acid, oxidation, carbamylation, dehydration, deamidation, dihydroxy, carboxymethyl and amidination (Fig. 14).

Co-/post-translational processing of *T. brucei* telomerase reverse transcriptase

Our MS analysis revealed a list of PTMs that compose both spontaneous modifications (oxidation) and ones that require an enzyme for their addition to proteins (N-terminal acetylation). We have identified the PF *Tb*TERT protein to undergo N-terminal acetylation, which is one of the most abundant post-translational modifications found in eukaryotes (Ree et al., 2018). N-terminal acetylation can proceed through two main pathways: the terminal methionine can be directly acetylated, or the methionine can be cleaved, and the second amino acid undergoes acetylation (Arnesen, 2011; Ree et al., 2018). Our mass spectrometry analysis revealed that the *Tb*TERT protein undergoes N-terminal acetylation (Fig. 12). The mass spectrometry analysis identified no peptides where the terminal methionine was directly acetylated. This indicates that there was complete excision of the terminal methionine followed by acetylation of the second amino acid residue alanine (Fig. 12**)**. All N-terminal peptide reads

identified by mass spectrometry showed terminal methionine cleavage followed by alanine acetylation.

3.4 Discussion

Protozoan parasites like *T. brucei* rely on constant telomerase activity to sustain high levels of cell division, which is necessary for the parasite to establish a chronic infection inside its host. Studying core interacting proteins in *T. brucei* telomerase is necessary to highlight potential novel mechanisms of telomerase regulation in these parasites. *T. brucei* undergoes a complex life cycle where it will differentiate into distinct developmental stages in its insect and human hosts respectively. Because of this, *T. brucei* allows for the study of the telomerase interactome across the parasite's life cycle. Here, using a mass spectrometry-based approach, we have identified the interactome of telomerase in the PF stage of *T. brucei* and identified the first PTMs of TERT in these parasites.

Some potential limitations of this study include the use antibody-based pulldown methods and the use of an overexpression system. No cross-linking of protein complexes were performed during these experiments meaning weaker or more transient interactions may be missed by this analysis. This may be one reason why there were no significant differences between BF and PF interactomes with regards to highly enriched candidate interactors. Also, the use of an overexpression system to express PF *Tb*TERT above endogenous levels may lead to changes in abundance and turnover rates of proteins because of more protein present in the cell, compared to endogenous levels. However, shared interactions between the two developmental stages of *T. brucei* lead to confidence in the presented approach to reliable detect TERT interacting proteins.

Our proteomics screen of the PF of *T. brucei* showed many conserved candidate interactors compared to the BF TERT interactome (Fig. 11). These interactors included proteins involved in DNA replication/repair, chaperones, and core C/D snoRNP. Similar pathways have also been identified in the BF TERT interactome and TERT interactomes from yeast (Davis et

al., 2023; Lin et al., 2015). Several chaperones were also identified in our analysis including the mitochondrial chaperone HSP60. HSP60 has been previously identified as an interactor of human TERT (Sharma et al., 2012). This interactor was also previously identified in the BF TERT interactome (Davis. et al., 2023). This conservation may indicate that a pool of *Tb*TERT localizes to the mitochondria in both *T. brucei* developmental stages. This dual-stage localization may also indicate a noncanonical role for *Tb*TERT protein in the mitochondria that is important for the biology of both developmental stages. There is precedent for this where human TERT has been shown to localize to the mitochondria under oxidative stress and play a noncanonical role beyond telomere maintenance (Ahmed et al., 2008; Sharma et al., 2012).

Core C/D box snoRNPs were also identified in our PF *Tb*TERT interactome. These proteins included core C/D box binding proteins like NOP58 and fibrillarin (NOP1) (Fig. 11). These proteins have also been previously identified to interact with *Tb*TERT in the BF developmental stage of this parasite (Davis et al., 2023; Gupta et al., 2013). This conservation of interactions between the BF and PF developmental stages suggests C/D box snoRNPs play important roles in TR processing and biogenesis in both developmental stages of *T. brucei*.

We also used our IP samples to map PF *Tb*TERT PTMs in an unbiased manner. We were able to identify 30 novel modification sites in *Tb*TERT (Fig. 14). These are the first PTMs of telomerase reported in *T. brucei* and they occur throughout the *Tb*TERT protein and localize to important TERT functional domains (Fig. 13). These modifications included a novel N-terminal acetylation site (Fig. 12). This is the first report of N-terminal acetylation of telomerase in any eukaryote. N-terminal acetylation is one of the most common PTMs observed in eukaryotes and has been implicated in protein stability, folding and cellular localization (Ree et al., 2018).

Common PTMs like phosphorylation could not be identified in this analysis. There are a few possible explanations for this observation. One, PF *Tb*TERT does not undergo extensive phosphorylation so sites could not be identified. PTMs generally exist in low stochiometric ratios that make detection by mass spectrometry a challenge. Because of this, enrichment strategies are usually employed to look at one PTM at a time to maximize chances of detection. Our study provides an unbiased list of PF *Tb*TERT PTMs that were able to be detected without enrichment.

The work described here provides the first analysis of the PF *Tb*TERT interactome and provides the first list of PTMs identified on *Tb*TERT. Our study lays the foundation for future studies of telomerase regulation in *T. brucei*. Future improvements are needed to refine the interactome present here. More transient interactions may be missed by this analysis and future studies will benefit from using a cross-linking approach to stabilize TERT interaction *in vivo*.

3.5 Figures

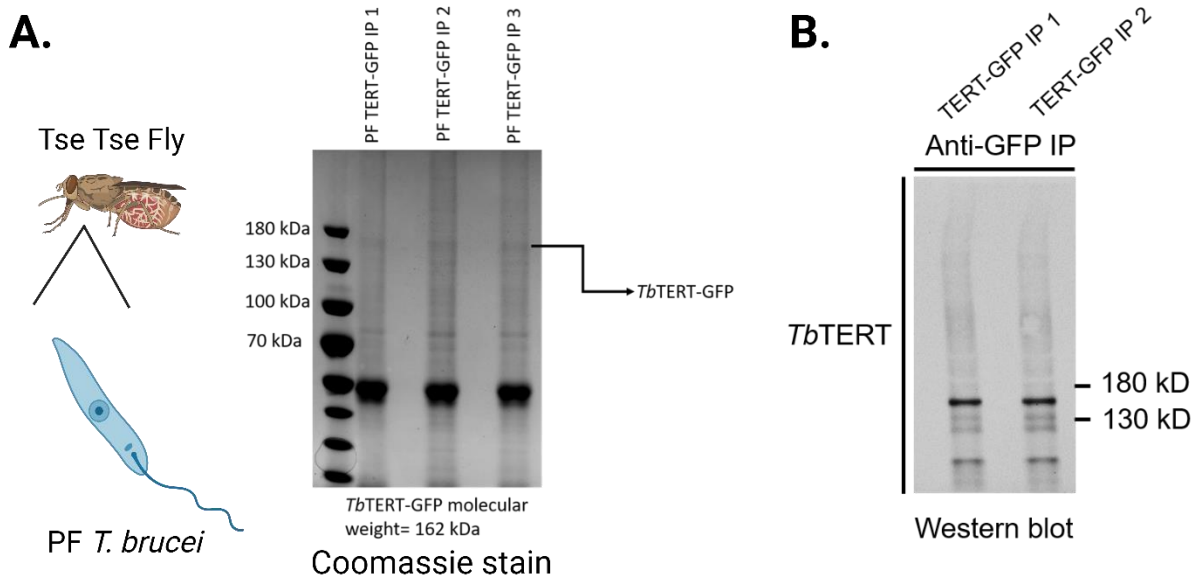

Figure 10. Affinity purification of PF *Tb*TERT-GFP. (A) SDS-PAGE gel analysis of PF *Tb*TERT-GFP IP elution's. A small aliquot of IP elution's was analyzed by SDS-PAGE and stained with Coomassie stain to qualitatively check *Tb*TERT-GFP protein levels. (B) Western blotting analysis to confirm the presence of immunopurified *Tb*TERT-GFP. *Tb*TERT-GFP was pulled down using an anti-GFP antibody and immunoblotted using an anti-C terminus *Tb*TERT antibody.

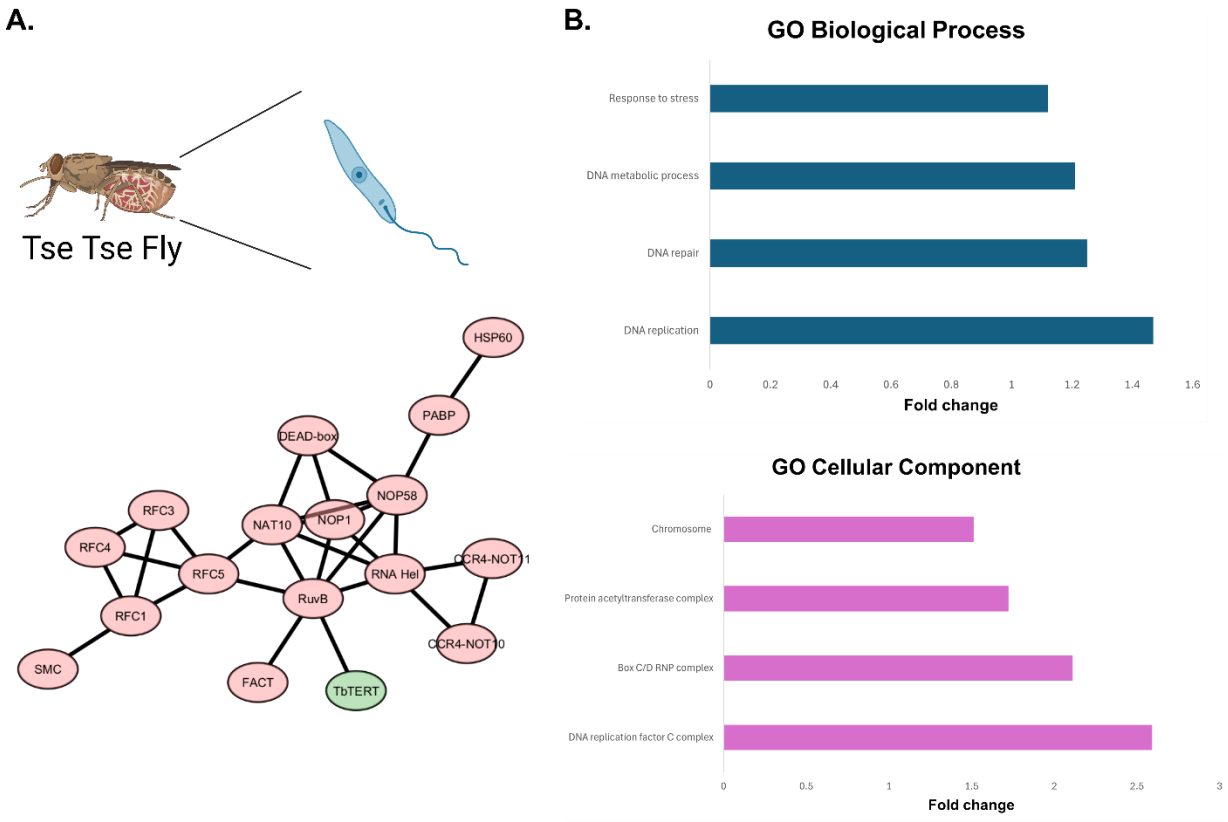

Figure 11. Interactome analysis of PF *Tb*TERT. (A) Protein-protein interaction network of the relevant interactors of *Tb*TERT identified by MS. Protein interaction network was generated using the STRING database and visualized using cytoscape. (B) STRING Gene ontology (GO) analysis of the PF *Tb*TERT interactome. Top graph shows terms related to biological process and bottom graph shows term related to cellular component. The top four hits are shown and a minimum fold change of one was used as a cut-off.

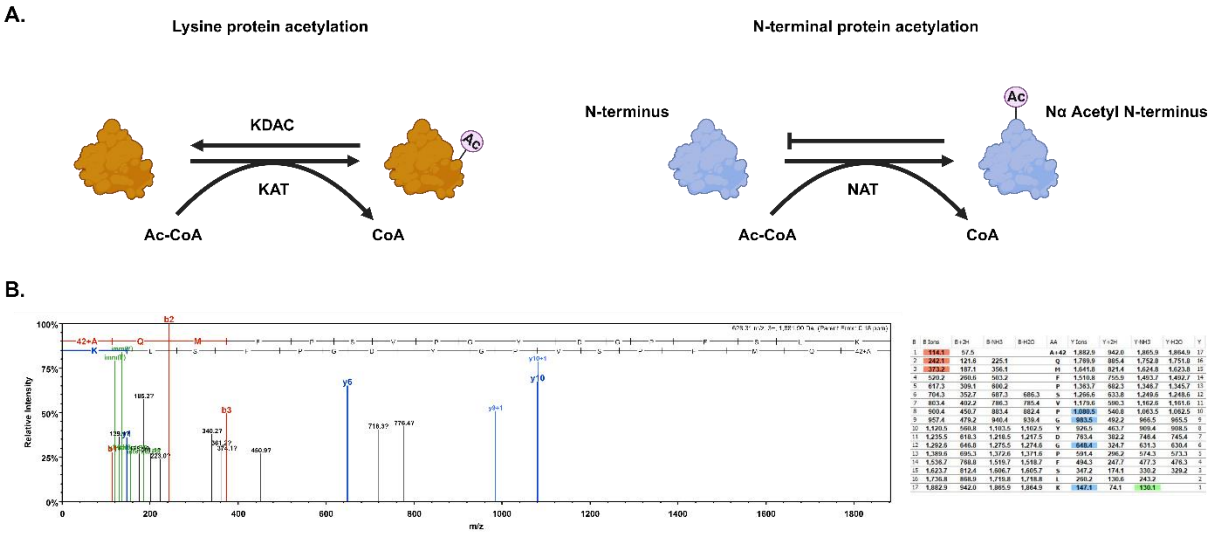

Figure 12. PF *Tb*TERT-GFP is N-terminally acetylated. (A) Comparison of normal lysine acetylation versus N-terminal acetylation. Lysine acetylation is a dynamic and reversible modification while N-terminal acetylation is irreversible. (B) MS2 spectrum showing N-methionine excision and N-acetylation of the proceeding alanine residue. +42 Da addition confirms the addition of an acetyl group to the terminal alanine.

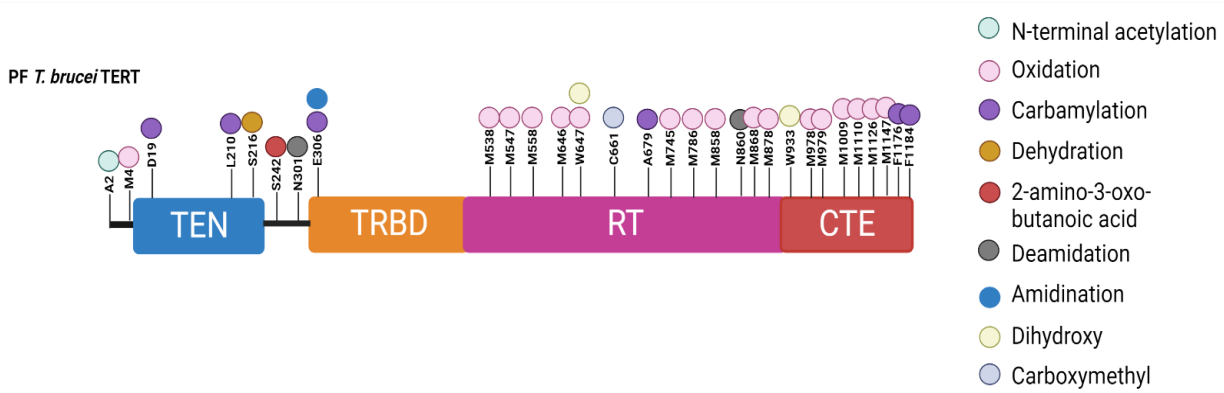

Figure 13. Map of PTMs on PF *Tb*TERT. Map of the Identified modifications in this study occur throughout the different functional domains of the *Tb*TERT protein. TEN: telomerase N-terminal domain, TRBD: telomerase RNA-binding domain, RT: reverse transcriptase catalytic domain, CTE: C-terminal extension domain.

Modified site	PTM
A2	N-term acetylation
M4	Oxidation
D19	Carbamylation
L210	Carbamylation
S216	Dehydration
S242	2-amino-3-oxo-butanoic acid
N301	Deamidation
E306	Amidination, Carbamylation
M538	Oxidation
M547	Oxidation
M558	Oxidation
M646	Oxidation
W647	Oxidation, Dihydroxy
C661	Carboxymethyl
A679	Carbamylation
M745	Oxidation
M786	Oxidation
M858	Oxidation
N860	Deamidation
M868	Oxidation
M878	Oxidation
W933	Dihydroxy
M978	Oxidation
M979	Oxidation
M1009	Oxidation
M1110	Oxidation
M1126	Oxidation
M1147	Oxidation
F1176	Carbamylation
F1184	Carbamylation

Figure 14. Table of modifications and modified sites identified in the PF *Tb*TERT protein.

CHAPTER 4: ROLES OF THE NOVEL TELOMERASE RNA DOMAINS (C/D BOX AND HELIX IV) IN TERT INTERACTION AND TELOMERASE REGULATION IN *TRYPANSOMA BRUCEI*

4.1 Introduction

Telomeres are the DNA-protein complexes found at the ends of eukaryotic linear chromosomes. Telomeres, and their associated binding proteins, form protective caps on the ends of chromosomes to protect genome integrity. Telomeres also function to prevent the 3' telomeric DNA overhang from being recognized as DNA damage inside the cell (Marcand, 2014). If telomeric DNA is falsely recognized as DNA damage, it can lead to the activation of the non-homologues end joining (NHEJ) pathway and telomeric fusions. These fused chromosomes can break and become damaged when the cell tries to replicate its DNA leading to DNA damage and genome instability. Telomeric shortening is also a prominent threat to genome integrity that eukaryotic organisms face. This telomeric shortening arises from the fact that DNA polymerases are unable to fully replicate the chromosomes completely to the ends. The actions of the RNA-protein enzyme telomerase solve the cells "end-replication problem" by maintaining telomere length (Chan & Blackburn, 2004). The telomerase enzyme consists of two main components necessary for telomerase activity *in vitro*. The two components are: the Telomerase Reverse Transcriptase (TERT) protein, which is the catalytic protein component, and the Telomerase RNA (TR) that provides the RNA template for telomere synthesis (Greider & Blackburn, 1985, 1989).

The TERT protein is highly conserved across a variety of eukaryotic species (Davis & Chakrabarti, 2022). The TR is the most divergent component of the telomerase enzyme across eukaryotes. The TR molecule acts as a structural scaffold in the telomerase holoenzyme and can differ in both size, structure, and sequence composition across different eukaryotic species (Dey

& Chakrabarti, 2018). RNAs, like proteins, can have important structural domains that carry out distinct functions (Fig. 3). The key structural domains found in the TR are the Template region, Template Boundary Element (TBE), Pseudoknot (PK) and the Stem Terminus Element (STE) (Egan & Collins, 2012). In mammalian cells, the STE is referred to as the CR4/5 domain (Chen et al., 2000; Kim et al., 2014). The CR4/5 domain is a well conserved feature of TR structure across a variety of eukaryotes (Davis & Chakrabarti 2022). The template region, and important TR structural domains, form a conserved region in the TR called the catalytic core. These core regions and motifs are required for telomerase catalytic activity inside the cell. These distinct RNA structural elements carry out specific roles with regards to telomerase regulation *in vivo*. The TBE elements are a highly conserved domain across eukaryotic TRs and are found near the template region. The TBE functions to demarcate the template region from the rest of the TR molecule. This domain functions to inhibit telomerase from adding nucleotides outside the template domain. This is critical as it preserves the correct sequence of the telomeric repeat and prevents mutations from being introduced into the telomeric sequence (Chen & Greider, 2003). The CR4/5 domain in the TR forms an important binding site in the TR molecule and is required for TERT binding to the TR (Mason et al., 2003). This interaction is critical for the proper assembly of a functional telomerase holoenzyme inside the cell. In addition to important structural domains, several TRs also contain important sequence motifs that serve as hotspots for interactions with RNA-binding proteins. A well-studied example of this is the H/ACA box small nucleolar RNA (snoRNA) domain found in mammalian TR. The canonical function of H/ACA box snoRNAs is in the processing and modifications of ribosomal RNAs (rRNAs) (Watkins & Bohnsack, 2012). The H/ACA box domain exists in the TR as a sequence motif that can bind core H/ACA box binding proteins. These proteins include: dyskerin, NHP2, GAR1 and NOP10.

These core H/ACA box binding proteins function to regulate TR processing and telomerase biogenesis and assembly in mammalian cells (Nguyen et al., 2018).

Trypanosoma brucei (*T. brucei*) is the protozoan parasite that causes African sleeping sickness in humans. This parasite has an intricate life cycle where it will transition between an insect host, the Tse Tse fly (*Glossina spp*.), which is the vector for the disease and a human host. During this time the parasite will transition between distinct developmental stages. The main two developmental stages include: the procyclic form (PF) found in the insect's midgut, and the bloodstream form (BF) found in the host's bloodstream. The BF form of this parasite is responsible for causing the symptoms associated with African sleeping sickness. *T. brucei* relies on constant telomerase activity to sustain high levels of cell division to establish a successful infection in its host. Telomerase regulation, including the structure and function of the TR, have been well studied in mammalian, yeast and *Tetrahymena* systems. Telomerase regulation is less understood in protozoan parasites like *T. brucei*. Recent studies have begun to illuminate aspects of telomerase regulation in *T. brucei*. The secondary structure of the TR catalytic core in *T. brucei* has been determined (Dey et al., 2021; Podlevsky et al., 2016; Sandhu et al., 2013). These studies showed that *T. brucei* TR (*Tb*TR) contains conserved and novel structural domains. These include a conserved catalytic core, and a homolog of the mammalian CR4/5 domain termed the Helix IV region in kinetoplastid parasites. The TR in *T. brucei* also contains novel elements like the presence of a C/D box snoRNA domain and a novel template distal helix domain (Dey et al., 2021; Gupta et al., 2013). The C/D box domain present in *T. brucei* replaces the H/ACA box domain observed in mammalian TRs. The C/D box domain is also found in closely related kinetoplastid parasites like *Leishmania* (Vasconcelos et al., 2014). The C/D box domain in *Tb*TR has been shown to bind core C/D box binding proteins like NOP58, Fibrillarin

(NOP1) and NOP56 (Davis et al., 2023; Gupta et al., 2013)**.** The novel interactions and structural domains found in the *Tb*TR suggest mechanistic differences in telomerase regulation in *T. brucei* compared to other eukaryotes and the species-specific functions of the Helix IV and C/D box domain are unknown in *T. brucei*.

To gain mechanistic insight into TR function and regulation in *T. brucei*, we have systematically deleted important structural domains in the *Tb*TR to probe the roles these domains play in regulating TR stability and telomerase catalytic activity. We have also begun to apply the glmS ribozyme-based system to generate conditional knockdown mutants in *T. brucei*. This system has been previously used in *T. brucei* to generate robust knockdown of expression of select target genes (Cruz-Bustos et al., 2018). We have begun to apply this system to tag and target the NOP58 gene to create a NOP58 conditional knockdown mutant in *T. brucei*. The goal of this system will be to downregulate NOP58 gene expression and probe the effects on *Tb*TR stability and folding using a combination of our RNA stability assays and SHAPE technology. We have highlighted the roles of important TR structural domains like the C/D box in telomerase regulation in these parasites. Understanding novel aspects of telomerase regulation in *T. brucei* lay the foundations for future studies to develop therapeutics that target novel telomerase regulatory pathways that only exist in *T. brucei* as a novel approach to treat African sleeping sickness in humans.

4.2 Materials and Methods

Culture of bloodstream form (BF) T. brucei cells

T. brucei Lister strain 427 was used throughout this study. All BF cells were grown in HMI-9 media supplemented with 10% heat inactivated Fetal Bovine Serum (FBS) at 37°C and 5% CO2. *T. brucei* Lister 427 strain expressing the T7 polymerase and Tet repressor (single marker, AKA SM) (Wirtz et al., 1999) was grown in media containing 2 μg/mL of G418; *Tb*TERT-FLAG-HA-HA (F2H) cells grown with 2 μg/mL of G418, 0.1 μg/mL Puromycin; *Tb*TR ΔC/D box, ΔTemplate, ΔHelix IV and ΔTBE mutant cells were grown with 2 μg/mL of G418, 4 μg/mL of Hygromycin, 2.5 μg/mL of Phleomycin, 5 μg/mL of Blasticidin, 0.1 μg/mL of Puromycin and 0.1 μg/mL of Doxycycline to constitutively induce the *Tb*TR mutations. ΔTERT cells were grown with 2 μg/mL of G418, .1 μg/mL of Puromycin and 5 μg/mL of Hygromycin. ΔTR cells were grown in the presence of 2 μg/mL of G418, 5 μg/mL Hygromycin and 5 μg/mL of Blasticidin.

Actinomycin D based RNA stability assay and qPCR

BF WT and mutant *T. brucei* cells were grown as described above. Cells were then treated with 10 μg/mL of actinomycin D to inhibit transcription and cells were collected every two hours for six hours (t= 0 hrs. untreated, t= 2, t= 4 hrs. and t= 6 hrs.). Following cell collection, total RNA was then extracted from the cells at the different time points using the TRIzol reagent (Thermo Fisher Scientific, 15596026) following the manufacturers protocol. Total RNA was then treated with TURBO DNase to remove any genomic DNA contamination per the manufactures protocol. 100 ng of total RNA from WT and mutant cells was then used for cDNA synthesis using the SuperScript II reverse transcriptase (Thermo Fisher Scientific,

18064022) following the manufacturers protocol. The generated cDNA was then used for qRT-PCR analysis using *Tb*TR specific primers (Fwd: CTGTGGAAATTTGTCGTAAGTG, Rev: AGTAGGGTTAGGGATCGTATAG). Decay curves were then plotted using the GraphPad Prism software. TR half-life was then calculated as the intercept on the X-axis at 50% decay of the TR molecule.

Immunopurification of T. brucei telomerase complexes for functional assays

Immunopurification of WT, ΔC/D box, ΔTemplate, ΔHelix IV and ΔTBE complexes was performed using Pierce Anti-DYKDDDDK magnetic beads (A36797). Approximately 6 × 108 cells/300 mL were harvested and lysed in 300 μL of immunopurified (IP) lysis buffer (25 mM Tris-HCl pH 7.5, 150 mM KCl, 25 mM NaCl, 1 mM EDTA, 10 mM MgCl2, 0.5% IGEPAL CA630, 1× protease cocktail inhibitor and 20 units of Ribolock RNase inhibitor). Lysate was cleared of debris by centrifugation at 3,000 rpm for 5 min at 4°C and incubated with pre-washed 50 μL of Pierce Anti-DYKDDDDK magnetic beads (A36797) at 4°C for 2 h with rotation. Following incubation, the beads were washed three times in ice cold IP buffer and once with ice cold DEPC water. The beads were then resuspended in 50 μL of RNAse free water.

Telomerase activity assay

To determine the activity of the Immunopurified *T. brucei* telomerase complexes from WT and mutant cells, a modified version of the exponential isothermal amplification of telomere repeat (EXPIATR) assay was performed (Dey et al., 2021; Tian & Weizmann, 2013) Briefly, reactions were prepared on ice consisting of Nicking Telomerase Substrate (NTS, GTGCGTGAGAGCTCTTCCAATCCGTCGAGC AGAGTT), Nicking Probe (NP,

AGCAGGAAGCGCTCTTCCTGC TCCCTAACCCTAACCC), 1X EXPIATR buffer (30 mM Tris-HCl, pH 8.3, 1.5 mM MgCl2, 100 mM KCl, 1 mM EGTA, 0.05% v/v Tween20), 200 µM dNTPs, Bst 2.0 Warm start DNA polymerase (0.96 units) and Nt. BspQ1 NEase (5 units). 17 µL of the master mix was aliquoted to PCR tubes containing, 3 µL of anti-FLAG or protein G bead bound *T. brucei* telomerase complexes, telomerase positive control (TPC8, GTGCGTGAGAGCTCTTCCAATCCGTCGAGCAGAGTTAGG GTTAGGGTTAGGGTTAGGGTTAGGGTTAGGGTTAGGGTT AGGG) (0.5 µM) and blank beads as a negative control. Telomerase activity was initiated by initial incubation of tubes at 28° C for 45 min for Nicking telomerase substrate (NTS) extension followed by amplification of resultant telomerase products at 55° C for 30 min. The amplified products were then analyzed on 12% Native PAGE gel. Densitometric analysis of the gel was carried out using the ImageJ software (National Institutes of Health, Maryland, USA) and relative telomerase activity was measured as the intensity of telomerase extension ladders. Mutant telomerase activity was normalized to the WT. Reactions were performed in biological duplicate (n= 2) and a one-way ANOVA test was then performed with Dunnett's multiple comparisons test to evaluate the statistical significance of the data. The P-values are reported in the figure legend.

Generation of T. brucei NOP58-glmS-HA cells

The pMOTag-glmS/M9-HA plasmids were kindly provided by the Docampo lab at the University of Georgia. The pMOTag-glmS-HA plasmid was used as a template and PCR was done to amplify the glmS-HA containing regions using Phusion high fidelity DNA polymerase. This amplified region was then purified from a 1% agarose gel using the GeneJET gel extraction kit following the manufactures protocol. This purified DNA was then used in a subsequent PCR

using NOP58 ultramers to add homology arms for integration. These PCR reactions were then scaled up (500 ul) and donor DNA was purified using phenol-chloroform extraction followed by ethanol precipitation. This donor DNA was then used to transfect BF cells similar to (Cruz-Bustos et al., 2018). Transfected cells were grown in the presence of 5 µg/mL of hygromycin to select for positive clones. Tagging of the endogenous NOP58 gene was then assayed by PCR.

4.3 Results

RNA stability in Telomerase RNA domain deletion mutants in T. brucei

The telomerase RNA (TR) molecule consists of various structural domains. These RNA structural domains, like protein domains, are distinct regions in RNA molecules that can perform different functions. RNA molecules, like the TR, need to be stabilized inside the cell so they can perform their biological roles. We first wanted to determine which TR structural domains are required for stability inside the cell and which were not. We tested this by generating mutant *T. brucei* cells that lack different TR structural domains. We then performed an RNA stability assay in WT and mutant cells to measure TR half-life. Our preliminary studies have indicated that knockdown of Telomerase RNA (TR) domains may result in differential accumulation of TR in *T. brucei* cells. To determine if these differences in RNA levels were due to changes in TR stability, we measured the decay of TR following inhibition of transcription with actinomycin D. We treated cells using the antibiotic actinomycin D, which is an intercalating agent that blocks RNA transcription, and took time points every two hours to measure TR abundance at each time point by qPCR. We generated TR mutants that had deletions of the: template region (Δtemplate), template boundary element (ΔTBE), C/D box domain (ΔC/D box) and the Helix IV (ΔHelix IV) domain. From our RNA stability assay, we determined the *in vivo* half-life of the WT TR in *T. brucei* to be approximately 6 hours (Fig. 15**)**. The stability of coding versus noncoding RNA can vary widely inside the cell (Clark et al., 2012). The stability of the *Tb*TR molecule is comparable to the stability of other long noncoding RNAs but certainly shorter than the previously observed telomerase RNA half-life in fission yeast (Hu et al., 2020). This assay was repeated in the TR mutant cells, and we found the TR stability was greatly reduced in the, ΔC/D box (t1/2≈ 1.2 hrs), Δtemplate (t1/2≈ 2 hrs), and the ΔHelix IV (t1/2≈ 1.8 hrs) mutant cells (Fig. 15**)**. The only TR mutant tested that did not have a significant effect on TR stability was the ΔTBE mutant (t1/2≈

5.8 hrs) whose TR half-life was comparable to WT cells (Fig. 15C**)**. Taken together, these results highlight there are structural domains within the TR that are essential for its stability and ones that are dispensable for its stability inside the cell.

The telomerase RNA in T. brucei is stable independent of its interactions with the telomerase reverse transcriptase protein

The TERT protein is not an essential gene in *T. brucei* (Dreesen & Li, 2005). Previous work has shown that the binding of the TERT protein in *T. brucei* has no role in the folding of the TR (Dey et al., 2021). We wanted to ask a related question and determine if TERT protein binding was required for TR stability inside the cell. We generated mutant *T. brucei* cells where the TERT protein is deleted (ΔTERT). To determine the stability of the TR in these mutant cells, we repeated the actinomycin D based RNA stability assay as described above. We found that the half-life of the TR was not signifcantly affected in the ΔTERT (t1/2≈ 6 hrs) (Fig. 16). These results demonstrate that in *T. brucei*, the TERT's interaction with the TR is not required for TR stability *in vivo*.

Deletion of the C/D box domain and Helix IV lead to a reduction in telomerase catalytic activity

The TR molecule is an integral part of the telomerase complex, which is essential for the enzyme's catalytic activity. We next wanted to test if deletion of TR structural domains affects telomerase catalytic activity. Telomerase activity *in vitro* was detected using a variation of the EXPIATR protocol (Dey et al., 2021; Tian & Weizmann, 2013) following immunopurification of *T. brucei* telomerase complexes from WT and mutant cells. Telomerase activity was

measured from WT, ΔTR, ΔC/D box and ΔHelix IV cells. Telomerase complexes from WT cells exhibited normal enzymatic activity (Fig. 17). This is in contrast to the ΔC/D box deletion cells, which exhibited a significant reduction in telomerase activity compared to the WT samples (Fig. 17). We then repeated this analysis in the ΔHelix IV cells and saw a significant decrease in telomerase catalytic activity from these cells (Fig. 17). Telomerase specific activity was confirmed by runing a negative control (blank beads) and no detectable telomerase activity was detected. The *Tb*TR domain deletion mutants also served as an internal control to demonstrate that observed activity is depenedt on the *Tb*TR molecule. These controls together deomonstrate that the observed primer extesions were due to the actions of the telomerase enzyme. Together, these results illustrate that deletion of structural domains within the TR molecule have implications for telomerase catalytic activty *in vitro*.

Conditional knockdown of T. brucei NOP58 to study RNA chaperone function

Conditional gene knockdowns can be a strong molecular biology tool to study the functions of proteins. Conditional knockdown using the glmS ribozyme system has been demonstrated to work effectively in *T. brucei* cells (Cruz-Bustos et al., 2018). Where, the endogenous gene is tagged at the 3' end with an HA tag and the glmS ribozyme. Gene knockdown can be triggered when glucosamine is added to the growth media to induce ribozyme activty. This leads to degredation of the target mRNA and downregulation of gene expression. We have begun to apply this system in our lab to generate conditonal knockdown mutants in T. *brucei* (Fig. 18A). We have succesful used the pMOTag-glmS-HA plamsid as a template to amplify the glmS-HA specific region and used this to generate NOP58 donor DNA (Fig. 18B).

We have performed preliminary transfections of BF *T. brucei* cells with this donor DNA and saw no integration into the genome (Fig. 18B).

4.4 Discussion

The activity of telomerase is critical to the success of a variety of eukaryotic microbes, including clinically relevant human parasites like *T. brucei*. *T. brucei* relies on constant telomerase activity to establish a successful chronic infection in its human host. The TR molecule is very divergent compared to its human counterpart and suggests mechanistic differences in telomerase regulation in *T. brucei* compared to humans. These discrepancies make telomerase a tempting target for the development of novel therapeutics targeting the TR, but the mechanisms of telomerase regulation are poorly understood in these parasites. We have systematically deleted structural domains in the *Tb*TR to gain novel insight into their roles in the regulation of telomerase in these parasites.

We first tested which TR structural domains are required for TR stability inside the cell. The domains assayed were the C/D box domain, Template region, TBE and the Helix IV region. Deletion of the TBE did not significantly affect the stability of the TR inside the cell (Fig. 15C). However, the other structural domains assayed, the C/D box domain, template domain and the Helix IV region all lead to a significant reduction in the stability of the TR *in vivo*. Thus, our results highlight essential and nonessential domains for TR stability in *T. brucei*. This allows us to generate a view of the TR in *T. brucei* where the TBE element is dispensable for TR stability inside the cell. Deletion of the C/D box, template region and Helix IV all lead to a reduction of TR stability, but we predict this loss of stability proceeds through distinct mechanisms depending on which domain is deleted. We also assayed if the TERT protein itself is required for TR stability in *T. brucei*. We found that deletion of the TERT protein does not lead to a significant reduction in TR stability in *T. brucei*. These results support earlier studies in *T. brucei* and other eukaryotes that TERT binding is not required for the proper folding of the TR *in vivo* (Dey et al., 2021; Richards et al., 2006). This data suggests that, in *T. brucei*, the TERT protein may not be

essential for the stability or folding of the TR *in vivo*. Because of this, we hypothesize that the template domain, which is essential for catalytic activity, Helix-IV, and the CD Box domain in *T. brucei* are essential structural elements required for stability, which would facilitate constant telomerase activity observed in these parasites.

To this end, we also wanted to determine if different structural domains in the TR are required for telomerase catalytic activity. We assayed telomerase activity in the ΔC/D box and ΔHelix IV cells and found a reduction of telomerase activity in both the ΔC/D box cells and ΔHelix IV cells. The Helix IV domain in *T. brucei* is a homolog of the CR4/5 domain found in mammalian cells (Chen et al., 2000; Kim et al., 2014). This domain has been well studied in mammalian cells and has been shown to be required for TERT binding and activity (Chen et al., 2002; Robart & Collins, 2010). Our results suggest that the Helix IV region in *Tb*TR plays a similar role in TERT binding and deletion of that domain leads to impaired TERT binding to the TR and a significant reduction in telomerase catalytic activity. The deletion of the ΔC/D box domain leads to a reduction in telomerase activity likely through a different mechanism. The C/D box in *T. brucei* replaces the H/ACA box in mammalian cells. These sequence motifs serve as prominent binding sites for core C/D and H/ACA snoRNPs in *T. brucei* and humans respectively (Davis et al., 2023; Egan & Collins, 2012b; Fu & Collins, 2003; Gupta et al., 2013). We hypothesize that the observed reduction in telomerase activity in the ΔC/D box mutant cells, arises from the destabilization of the TR in the absence of the C/D box domain.

Taken together, our results lead us to propose a model for the role of the novel C/D box snoRNA domain in *Tb*TR regulation shown in Figure 19. In this model, the end of the *Tb*TR molecule is capped by core C/D box snoRNPs binding to the C/D box domain. The binding of these C/D snoRNPs protect the end of the *Tb*TR inside the cell from being degraded by

endogenous exonucleases (Fig. 19). In contrast to WT, in ΔC/D box mutant cells, deletion of this domain leads to a loss of interaction with the C/D snoRNPs leading to loss of end protection and rapid degradation of the *Tb*TR inside the cell. Loss of binding between C/D snoRNPs in the absence of the C/D box has been previously reported (Davis et al., 2023) and we confirmed a drastic reduction in the stability of the *Tb*TR in ΔC/D box cells with our RNA stability assays. With our current understanding we cannot conclude if this degradation process proceeds through a specific exonuclease, like the CCR4-NOT complex, which has been recently shown to be a part of the *T. brucei* telomerase complex (Davis et al., 2023), or if it is a more general exonuclease driven process (Fig. 19). This proposed mechanism is consistent with previously reported end-protection mechanisms found in other long non-coding RNAs that have snoRNA ends (Yin et al., 2012).

Previously, we have shown that NOP58, a putative RNA chaperone is important for binding to *T. brucei* TR CD Box domain, potentially for proper biogenesis and folding of RNA (Figure 8). TR chaperones, like p65, have been identified in ciliates and have been shown to be required for proper TR folding. To understand if NOP58 acts as a chaperone for the *T. brucei* TR, we have taken an initiative to create a conditional knockdown of NOP58 protein using the glmS ribozyme system. We were successfully able to generate enough donor DNA for preliminary transfections. We performed a first round of transfections and observed no integration into the *T. brucei* genome (Fig. 18B). We will look to optimize these assays in the future by altering cell number and amount of donor DNA used as BF *T. brucei* cells are notoriously hard to transfect and show low transfection efficiency. This system will eventually be used to interrogate NOP58 role in *Tb*TR stability and folding using our RNA stability assays to determine stability of the TR after NOP58 downregulation. We will also seek to answer if

NOP58 binding is required for proper *Tb*TR folding inside the cell. NOP58 expression will be downregulated, and RNA SHAPE technology will be used to determine if structural changes are occurring in the *Tb*TR molecule when NOP58 expression is reduced. These studies will provide novel insight into the role of C/D box snoRNPs in telomerase regulation beyond what is presented here.

The work described here provides the first detailed analysis for the roles of various conserved and novel structural domains in the regulation of the *Tb*TR molecule. We were able to identify structural domains within the *Tb*TR molecule that were either essential or nonessential for the stability of the *Tb*TR molecule inside the cell. Our analysis also revealed that the TERT protein plays no role in stabilizing the *Tb*TR molecule. This is consistent with previous studies in *T. brucei* and other eukaryotes that the TERT protein also plays no role in the folding of the TR (Dey et al., 2021; Richards et al., 2006). Our work also highlights that destabilization of the *Tb*TR leads to a reduction in telomerase catalytic activity. These observations lead us to propose a role for the novel C/D box domain in *Tb*TR regulation. In our model, the C/D box motif at the end of the *Tb*TR molecule are bound by core C/D snoRNPs to form a protective cap on the TR to protect it from endogenous exonuclease degradation inside the cell. Taken together our results highlight novel aspects of telomerase regulation in *T. brucei* that do not exist in other eukaryotes whose TRs contain and H/ACA box domain. Our work provides the foundation for future studies on unique mechanisms of *T. brucei* telomerase regulation that can potentially be the target of novel therapeutics to treat this parasitic disease.

4.5 Figures

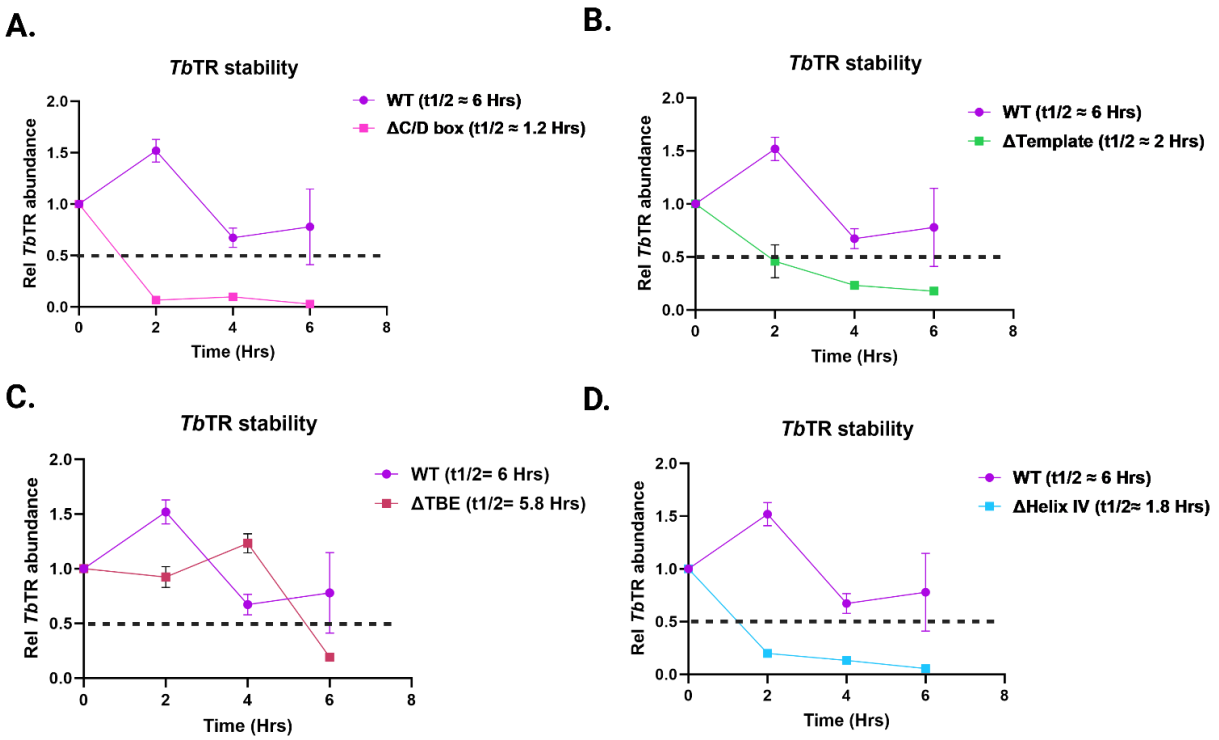

Figure 15. Role of various structural domains in *T. brucei* telomerase RNA stability. (A) TR degradation rates in WT versus ΔC/D box mutant cells. (B) TR degradation rates in WT versus ΔTemplate cells. (C) TR degradation rates in WT versus ΔTBE cells. (D) TR degradation rates in WT versus ΔHelix IV cells. Dots and Error bars represent the mean and SEM respectively from three technical replicates (n= 3).

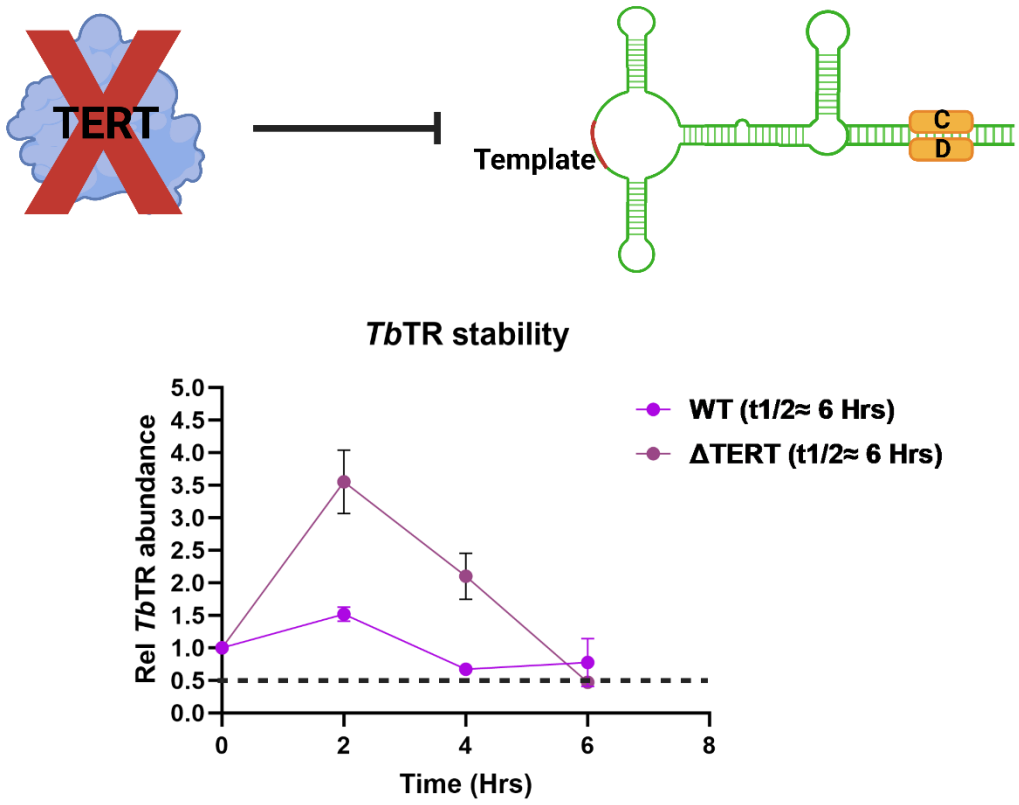

Figure 16. *Tb*TR is stable independent of its interactions with the TERT protein. TR degradation rates in WT versus ΔTERT cells. Dots and Error bars represent the mean and SEM respectively from three technical replicates (n= 3).

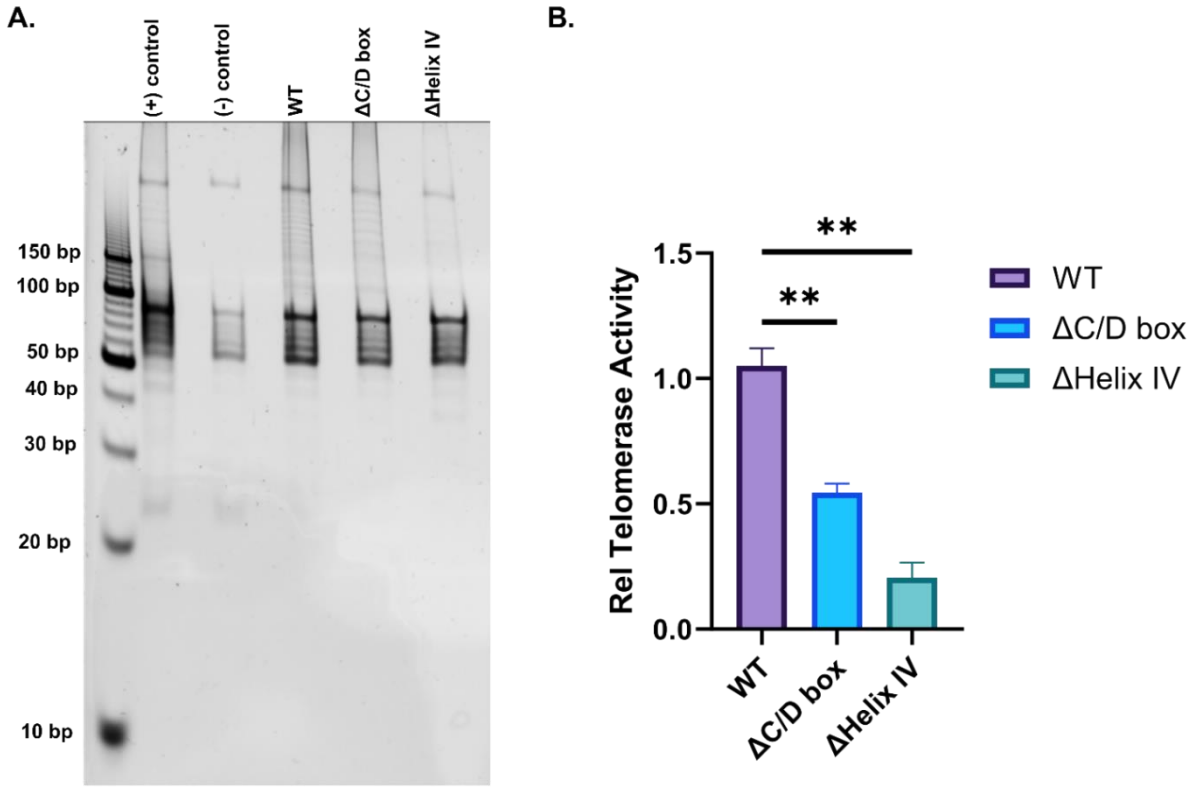

Figure 17. Loss of the C/D box and Helix IV domains lead to a reduction in *T. brucei* telomerase catalytic activity. (A) Telomerase activity in WT and mutant cells was assayed by telomerase primer extension assay. (B) Quantification of telomerase activity in (A), values were normalized to WT. Mean and standard deviation were derived from two independent experiments (n= 2). WT vs. ΔC/D box p-value= .0052, WT vs. ΔHelix IV p-value= .0011 by Dunnett's multiple comparison test.

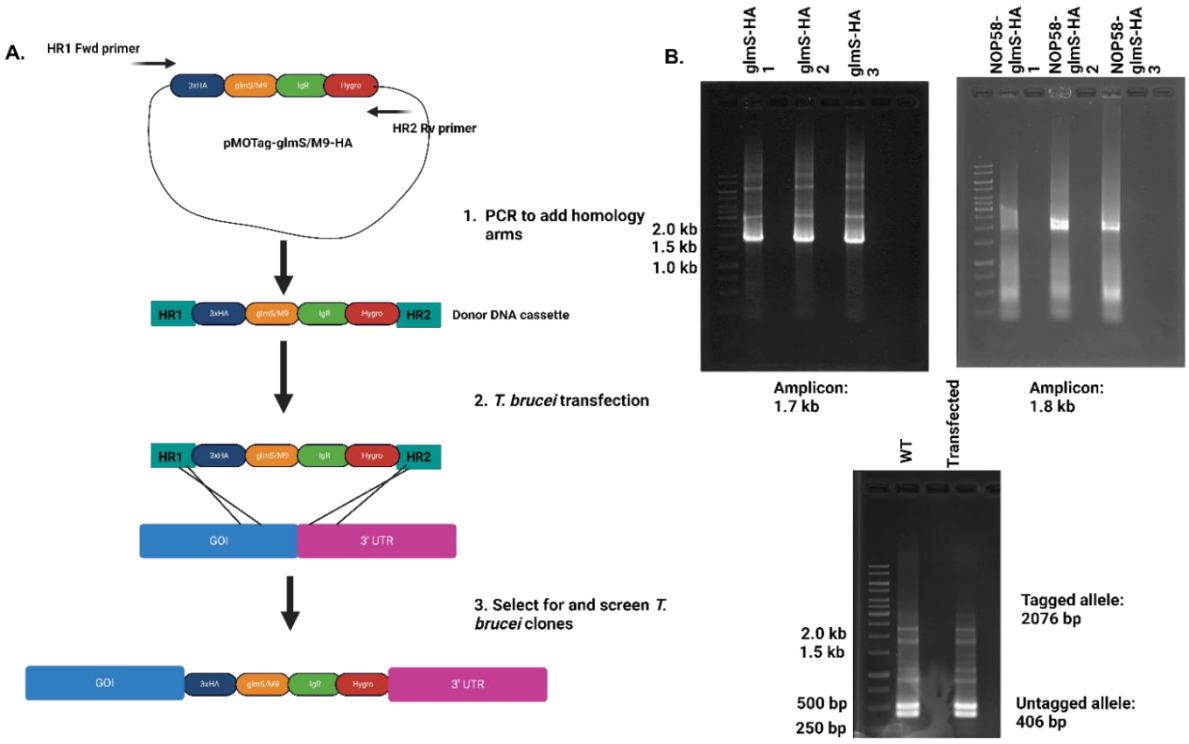

Figure 18. Generation of NOP58-glmS-HA conditional knockdown cell line. (A) Experimental workflow used to generate NOP58-glmS-HA *T. brucei* cells. (B, top) PCRs to amplify plasmid specific region and generate NOP58 donor DNA. (B, bottom) PCR to check for integration and tagging of the endogenous NOP58 locus.

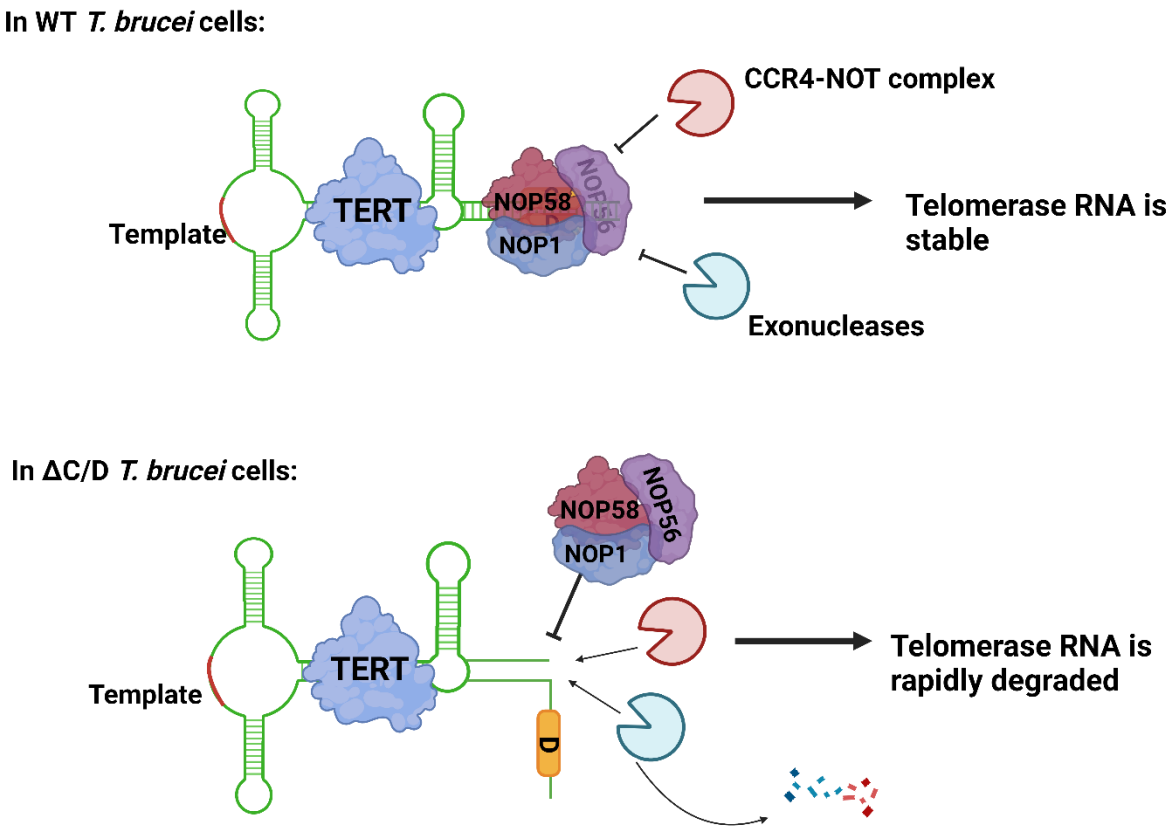

Figure 19. Putative role of the novel C/D box snoRNA domain in *Tb*TR regulation. In WT cells, the C/D box domain is bound by core C/D snoRNPs. This binding forms a protective cap on the end of the *Tb*TR molecule to block degradation by endogenous exonucleases inside the cell. This leads to a stabilization of the *Tb*TR molecule inside the cell. In ΔC/D box mutant cells, the interactions with the core C/D box snoRNPs are lost. This loss of binding leads to uncapping of the end of the *Tb*TR molecule and exposes the TR to exonuclease degradation. This leads to rapid degradation and destabilization of the *Tb*TR molecule inside the cell.

CHAPTER 5: CONCLUSIONS

In this dissertation, we have highlighted and characterized novel mechanisms of telomerase regulation that exist in the deep branching eukaryote, *T. brucei*. We have done this using a combination of proteomic and molecular biology techniques. We have reported the first global interactome of telomerase in *T. brucei* and have followed up on important protein interactions. We found that the telomerase complex in *T. brucei* Bloodstream Form (BF) is composed of conserved and novel protein interactors (Davis et al., 2023). These interactors include a core group of C/D snoRNPs like NOP58 (Fig. 8). These novel associations with core C/D box binding proteins are unique to *T. brucei* telomerase and absent in mammalian telomerase. Other core C/D snoRNPs were also identified in this study including NOP56 and fibrillarin (NOP1). These proteins have canonical roles in ribosomal RNA biogenesis and processing (Barth et al., 2008). These processes include addition of chemical modifications on to ribosomal RNAs that have been shown to regulate ribosomal RNA folding and function (Watkins & Bohnsack, 2012). Whether these proteins perform similar functions on the *Tb*TR remains to be explored. We have also identified the interactome *Tb*TERT in PF *T. brucei* cells. We found that core interacting proteins of telomerase were conserved between the two developmental stages (Fig. 11). These proteins include protein chaperones, like HSP60, and core C/D snoRNPs. The GO analysis of the PF *Tb*TERT interactome also highlighted many of the same pathways that were enriched in the BF interactome. These include processes involved in DNA replication/repair and RNA metabolism. The presence of core telomerase interacting proteins in both developmental stages of *T. brucei* highlights their importance in telomerase regulation and function in both BF and PF *T. brucei* cells. This global analysis gave us insights

into protein-protein and RNA-protein interactions that make up the telomerase holoenzyme in *T. brucei*.

Secondary structure determination of RNA is a valuable approach and a good starting point for in-depth mechanistic studies. Mapping RNA structure allows for identification of structural domains that are important for RNA function. Previously, Chakrabarti lab determined the secondary structure of telomerase RNA in *T. brucei* based on comparative genomics, sequence co-variation and *in vivo* mutational mapping (Dey et al., 2021; Sandhu et al., 2013). However, functional characterization of various domains in the *T. brucei* telomerase RNA structure remained unresolved. Therefore, to study the roles of various structural domains within the TR, their role in TR stability and telomerase catalytic activity, we used the following molecular and biochemical approaches. The approaches we used to determine this were a combination of RNA stability assays and telomerase activity assays. Using these approaches we found the C/D box, Helix IV and the template domains were all required for *Tb*TR stability inside the cell while the TBE domain was dispensable (Fig. 12). We were also able to demonstrate that destabilization of the *Tb*TR lead to a significant reduction in telomerase catalytic activity (Fig. 14). This data, and our initial interactome study, lead us to propose a mechanism for the C/D box domain in stabilizing the *Tb*TR inside the cell. In our proposed model, the C/D box domain is bound by core snoRNPs, like NOP58, that form a protective cap to block the RNA from being degraded by endogenous exonucleases inside the cell. Subsequent deletion of the C/D box domain, lead to a loss of interaction with the core C/D snoRNPs and the protective cap was lost. This then led to rapid degradation of the *Tb*TR molecule inside the cell (Fig. 15). This work provided novel mechanistic insight into telomerase regulation in *T. brucei*.

Telomerase activity is regulated through a variety of mechanisms including protein-protein and RNA-protein interactions. Another mechanism of telomerase regulation that has been reported is the addition of posttranslational modifications or PTMs. PTMs of TERT have been identified in human and yeast systems, but no modifications of telomerase have been reported in *T. brucei*. To address this knowledge gap, we immunopurified *Tb*TERT from PF cells and mapped the PTMs on the enzyme using mass spectrometry. We were able to identify 30 novel modified sites in *Tb*TERT including a novel N-terminal acetylation site. This N-terminal acetylation has not been reported on telomerase in any other eukaryotes.

This dissertation has highlighted and studied novel pathways of telomerase regulation in *T. brucei*. These novel insights and understandings have expanded our knowledge of telomerase biology in parasitic protozoa like *T. brucei*. Future directions will look to follow-up and further refine the work presented in this dissertation. It will be interesting to try and identify if the degradation of the *Tb*TR proceeds through a specific exonuclease or is a more general exonuclease driven process. It would also be interesting to repeat similar experiments in *Leishmania*. *Leishamnia* is a closely related parasite to *T. brucei* and the *Leishmania* TR also contains a C/D box domain. It would be easy to speculate that a similar mechanism may exist in *Leishmania* for TR end-protection and stabilization. This could represent a conserved mechanism in kinetoplastid parasites for TR stability and biogenesis. This novel mechanism could eventually be targeted for therapeutic development as it is unique to these parasites and absent in their human hosts. Other future experiments could focus on the functional roles for the telomerase modifications presented in this thesis. These specific residues, like the N-terminal acetylation site, could be mutated to address the biological roles these modifications play with respect to telomerase regulation in these parasites.

REFERENCES

Afrin, M., Gaurav, A. K., Yang, X., Pan, X. H., Zhao, Y. X., & Li, B. B. (2020). TbRAP1 has an unusual duplex DNA binding activity required for its telomere localization and VSG silencing. *Science Advances, 6*(38). https://doi.org/ARTN eabc4065
10.1126/sciadv.abc4065

Ale-Agha, N., Jakobs, P., Goy, C., Zurek, M., Rosen, J., Dyballa-Rukes, N., Metzger, S., Greulich, J., von Ameln, F., Eckermann, O., Unfried, K., Brack, F., Grandoch, M., Thielmann, M., Kamler, M., Gedik, N., Kleinbongard, P., Heinen, A., Heusch, G., . . . Haendeler, J. (2021). Mitochondrial Telomerase Reverse Transcriptase Protects From Myocardial Ischemia/Reperfusion Injury by Improving Complex I Composition and Function. *Circulation, 144*(23), 1876-1890. https://doi.org/10.1161/Circulationaha.120.051923

Amanda, J. Y., & Romero, D. P. (2002). A unique pause pattern during telomere addition by the error-prone telomerase from the ciliate Paramecium tetraurelia. *Gene, 294*(1-2), 205-213.

Arnesen, T. (2011). Towards a functional understanding of protein N-terminal acetylation. *PLoS biology, 9*(5), e1001074.

Barth, S., Shalem, B., Hury, A., Tkacz, I. D., Liang, X. H., Uliel, S., Myslyuk, I., Doniger, T., Salmon-Divon, M., Unger, R., & Michaeli, S. (2008). Elucidating the role of C/D snoRNA in rRNA processing and modification in Trypanosoma brucei. *Eukaryotic Cell, 7*(1), 86-101. https://doi.org/10.1128/Ec.00215-07

Bayisotto, C. C., Alberti, G., Vitale, A. M., Paladino, L., Campanella, C., Rappa, F., Gorska, M., de Macario, E. C., Cappello, F., Macario, A. J. L., & Gammazza, A. M. (2020). Hsp60 Post-translational Modifications: Functional and Pathological Consequences. *Frontiers in Molecular Biosciences, 7*. https://doi.org/ARTN 95
10.3389/fmolb.2020.00095

Benmerzouga, I., Concepcion-Acevedo, J., Kim, H. S., Vandoros, A. V., Cross, G. A. M., Klingbeil, M. M., & Li, B. B. (2013). Trypanosoma brucei Orc1 is essential for nuclear DNA replication and affects both VSG silencing and VSG switching. *Molecular Microbiology, 87*(1), 196-210. https://doi.org/10.1111/mmi.12093

Berman, A. J., Gooding, A. R., & Cech, T. R. (2010). Tetrahymena Telomerase Protein p65 Induces Conformational Changes throughout Telomerase RNA (TER) and Rescues Telomerase Reverse Transcriptase and TER Assembly Mutants. *Molecular and cellular biology, 30*(20), 4965-4976. https://doi.org/10.1128/Mcb.00827-10

Chan, S. R., & Blackburn, E. H. (2004). Telomeres and telomerase. *Philosophical Transactions of the Royal Society of London. Series B: Biological Sciences, 359*(1441), 109-122.

Chen, J.-L., Blasco, M. A., & Greider, C. W. (2000). Secondary structure of vertebrate telomerase RNA. *Cell, 100*(5), 503-514.

Chen, J.-L., & Greider, C. W. (2003). Template boundary definition in mammalian telomerase. *Genes & development, 17*(22), 2747-2752.

Chen, J.-L., Opperman, K. K., & Greider, C. W. (2002). A critical stem–loop structure in the CR4–CR5 domain of mammalian telomerase RNA. *Nucleic acids research, 30*(2), 592-597.

Chen, L., Roake, C. M., Freund, A., Batista, P. J., Tian, S., Yin, Y. A., Gajera, C. R., Lin, S., Lee, B., & Pech, M. F. (2018). An activity switch in human telomerase based on RNA conformation and shaped by TCAB1. *Cell*, *174*(1), 218-230. e213.

Choi, J.-H., Lindsey-Boltz, L. A., Kemp, M., Mason, A. C., Wold, M. S., & Sancar, A. (2010). Reconstitution of RPA-covered single-stranded DNA-activated ATR-Chk1 signaling. *Proceedings of the National Academy of Sciences*, *107*(31), 13660-13665.

Chung, J., Khadka, P., & Chung, I. K. (2012). Nuclear import of hTERT requires a bipartite nuclear localization signal and Akt-mediated phosphorylation. *Journal of cell science*, *125*(11), 2684-2697.

Clark, M. B., Johnston, R. L., Inostroza-Ponta, M., Fox, A. H., Fortini, E., Moscato, P., Dinger, M. E., & Mattick, J. S. (2012). Genome-wide analysis of long noncoding RNA stability. *Genome research*, *22*(5), 885-898.

Cohen, S. B., Graham, M. E., Lovrecz, G. O., Bache, N., Robinson, P. J., & Reddel, R. R. (2007). Protein composition of catalytically active human telomerase from immortal cells. *Science*, *315*(5820), 1850-1853.

Collins, K. (2006). The biogenesis and regulation of telomerase holoenzymes. *Nature reviews Molecular cell biology*, *7*(7), 484-494.

Cotobal, C., Rodriguez-Lopez, M., Duncan, C., Hasan, A., Yamashita, A., Yamamoto, M., Bahler, J., & Mata, J. (2015). Role of Ccr4-Not complex in heterochromatin formation at meiotic genes and subtelomeres in fission yeast. *Epigenetics & Chromatin*, *8*. https://doi.org/ARTN 28
10.1186/s13072-015-0018-4

Cracco, L., Doud, E. H., Hallinan, G. I., Garringer, H. J., Jacobsen, M. H., Richardson, R. M., Buratti, E., Vidal, R., Ghetti, B., & Newell, K. L. (2022). Distinguishing post-translational modifications in dominantly inherited frontotemporal dementias: FTLD-TDP Type A (GRN) vs Type B (C9orf72). *Neuropathology and Applied Neurobiology*, *48*(6), e12836.

Cruz-Bustos, T., Ramakrishnan, S., Cordeiro, C. D., Ahmed, M. A., & Docampo, R. (2018). A riboswitch-based inducible gene expression system for Trypanosoma brucei. *journal of eukaryotic microbiology*, *65*(3), 412-421.

Davis, J. A., & Chakrabarti, K. (2022). Telomerase ribonucleoprotein and genome integrity—An emerging connection in protozoan parasites. *Wiley Interdisciplinary Reviews: RNA*, *13*(5), e1710.

Davis, J. A., Reyes, A. V., Saha, A., Wolfgeher, D. J., Xu, S.-L., Truman, A. W., Li, B., & Chakrabarti, K. (2023). Proteomic analysis defines the interactome of telomerase in the protozoan parasite, Trypanosoma brucei. *Frontiers in Cell and Developmental Biology*, *11*, 1110423.

de Lange, T. (2018). Shelterin-mediated telomere protection. *Annual review of genetics*, *52*, 223-247.

De Lange, T., & Borst, P. (1982). Genomic environment of the expression-linked extra copies of genes for surface antigens of Trypanosoma brucei resembles the end of a chromosome. *Nature*, *299*(5882), 451-453.

Dey, A., & Chakrabarti, K. (2018). Current perspectives of telomerase structure and function in eukaryotes with emerging views on telomerase in human parasites. *International journal of molecular sciences*, *19*(2), 333.

Dey, A., Monroy-Eklund, A., Klotz, K., Saha, A., Davis, J., Li, B., Laederach, A., & Chakrabarti, K. (2021). In vivo architecture of the telomerase RNA catalytic core in Trypanosoma brucei. *Nucleic acids research*, *49*(21), 12445-12466.

Dreesen, O., & Cross, G. A. (2008). Telomere length in Trypanosoma brucei. *Experimental parasitology*, *118*(1), 103-110.

Dreesen, O., & Cross, G. A. M. (2006). Consequences of telomere shortening at an active VSG expression site in telomerase-deficient Trypanosoma brucei. *Eukaryotic Cell*, *5*(12), 2114-2119. https://doi.org/10.1128/Ec.00059-06

Dreesen, O., & Li, B. B. (2005). Telomere structure and shortening in telomerase-deficient Trypanosoma brucei. *Nucleic acids research*, *33*(14), 4536-4543. https://doi.org/10.1093/nar/gki769

Egan, E. D., & Collins, K. (2012a). Biogenesis of telomerase ribonucleoproteins. *Rna*, *18*(10), 1747-1759.

Egan, E. D., & Collins, K. (2012b). An enhanced H/ACA RNP assembly mechanism for human telomerase RNA. *Molecular and cellular biology*, *32*(13), 2428-2439.

Evans, S. K., & Lundblad, V. (2002). The Est1 subunit of Saccharomyces cerevisiae telomerase makes multiple contributions to telomere length maintenance. *Genetics*, *162*(3), 1101-1115.

Ferguson, J. L., Chao, W. C. H., Lee, E., & Friedman, K. L. (2013). The Anaphase Promoting Complex Contributes to the Degradation of the S. cerevisiae Telomerase Recruitment Subunit Est1p. *Plos One*, *8*(1). https://doi.org/ARTN e55055
10.1371/journal.pone.0055055

Fu, D., & Collins, K. (2003). Distinct biogenesis pathways for human telomerase RNA and H/ACA small nucleolar RNAs. *Molecular Cell*, *11*(5), 1361-1372.

Fu, D., & Collins, K. (2007). Purification of human telomerase complexes identifies factors involved in telomerase biogenesis and telomere length regulation. *Molecular Cell*, *28*(5), 773-785. https://doi.org/10.1016/j.molcel.2007.09.023

Greider, C. W. (1991). Telomerase is processive. *Molecular and cellular biology*.

Greider, C. W., & Blackburn, E. H. (1985). Identification of a specific telomere terminal transferase activity in Tetrahymena extracts. *Cell*, *43*(2), 405-413.

Greider, C. W., & Blackburn, E. H. (1989). A telomeric sequence in the RNA of Tetrahymena telomerase required for telomere repeat synthesis. *Nature*, *337*(6205), 331-337.

Gunisova, S., Elboher, E., Nosek, J., Gorkovoy, V., Brown, Y., Lucier, J.-F., Laterreur, N., Wellinger, R. J., Tzfati, Y., & Tomaska, L. (2009). Identification and comparative analysis of telomerase RNAs from Candida species reveal conservation of functional elements. *Rna*, *15*(4), 546-559.

Gupta, S. K., Kolet, L., Doniger, T., Biswas, V. K., Unger, R., Tzfati, Y., & Michaeli, S. (2013). The Trypanosoma brucei telomerase RNA (TER) homologue binds core proteins of the C/D snoRNA family. *FEBS letters*, *587*(9), 1399-1404.

Haendeler, J., Hoffmann, J., Brandes, R. P., Zeiher, A. M., & Dimmeler, S. (2003). Hydrogen peroxide triggers nuclear export of telomerase reverse transcriptase via Src kinase family-dependent phosphorylation of tyrosine 707. *Molecular and cellular biology*, *23*(13), 4598-4610.

Han, S., Zhao, B. S., Myers, S. A., Carr, S. A., He, C., & Ting, A. Y. (2020). RNA-protein interaction mapping via MS2-or Cas13-based APEX targeting. *Proceedings of the*

National Academy of Sciences of the United States of America, *117*(36), 22068-22079. https://doi.org/10.1073/pnas.2006617117

He, Y., Wang, Y. Q., Liu, B. C., Helmling, C., Susac, L., Cheng, R., Zhou, Z. H., & Feigon, J. (2021). Structures of telomerase at several steps of telomere repeat synthesis. *Nature*, *593*(7859), 454-+. https://doi.org/10.1038/s41586-021-03529-9

Holm, L., & Rosenstrom, P. (2010). Dali server: conservation mapping in 3D. *Nucleic acids research*, *38*, W545-W549. https://doi.org/10.1093/nar/gkq366

Holt, S. E., Aisner, D. L., Baur, J., Tesmer, V. M., Dy, M., Ouellette, M., Trager, J. B., Morin, G. B., Toft, D. O., Shay, J. W., Wright, W. E., & White, M. A. (1999). Functional requirement of p23 and Hsp90 in telomerase complexes. *Genes & development*, *13*(7), 817-826. https://doi.org/DOI 10.1101/gad.13.7.817

Hovel-Miner, G. A., Boothroyd, C. E., Mugnier, M., Dreesen, O., Cross, G. A. M., & Papavasiliou, F. N. (2012). Telomere Length Affects the Frequency and Mechanism of Antigenic Variation in Trypanosoma brucei. *Plos Pathogens*, *8*(8). https://doi.org/ARTN e1002900

10.1371/journal.ppat.1002900

Hu, X., Kim, J.-K., Yu, C., Jun, H.-I., Liu, J., Sankaran, B., Huang, L., & Qiao, F. (2020). Quality-control mechanism for telomerase RNA folding in the cell. *Cell reports*, *33*(13).

Indran, I. R., Hande, M. P., & Pervaiz, S. (2011). hTERT Overexpression Alleviates Intracellular ROS Production, Improves Mitochondrial Function, and Inhibits ROS-Mediated Apoptosis in Cancer Cells. *Cancer Research*, *71*(1), 266-276. https://doi.org/10.1158/0008-5472.Can-10-1588

Jehi, S. E., Nanavaty, V., & Li, B. B. (2016). Trypanosoma brucei TIF2 and TRF Suppress VSG Switching Using Overlapping and Independent Mechanisms. *Plos One*, *11*(6). https://doi.org/ARTN e0156746

10.1371/journal.pone.0156746

Jehi, S. E., Wu, F., & Li, B. B. (2014). Trypanosoma brucei TIF2 suppresses VSG switching by maintaining subtelomere integrity. *Cell research*, *24*(7), 870-885. https://doi.org/10.1038/cr.2014.60

Jiang, J., Chan, H., Cash, D. D., Miracco, E. J., Ogorzalek Loo, R. R., Upton, H. E., Cascio, D., O'Brien Johnson, R., Collins, K., & Loo, J. A. (2015). Structure of Tetrahymena telomerase reveals previously unknown subunits, functions, and interactions. *Science*, *350*(6260), aab4070.

Jiang, J., Miracco, E. J., Hong, K., Eckert, B., Chan, H., Cash, D. D., Min, B., Zhou, Z. H., Collins, K., & Feigon, J. (2013). The architecture of Tetrahymena telomerase holoenzyme. *Nature*, *496*(7444), 187-192.

Jumper, J., Evans, R., Pritzel, A., Green, T., Figurnov, M., Ronneberger, O., Tunyasuvunakool, K., Bates, R., Zidek, A., Potapenko, A., Bridgland, A., Meyer, C., Kohl, S. A. A., Ballard, A. J., Cowie, A., Romera-Paredes, B., Nikolov, S., Jain, R., Adler, J., . . . Hassabis, D. (2021). Highly accurate protein structure prediction with AlphaFold. *Nature*, *596*(7873), 583-+. https://doi.org/10.1038/s41586-021-03819-2

Jung, H.-Y., Wang, X., Jun, S., & Park, J.-I. (2013). Dyrk2-associated EDD-DDB1-VprBP E3 ligase inhibits telomerase by TERT degradation. *Journal of Biological Chemistry*, *288*(10), 7252-7262.

Jung, H. Y., Wang, X., Jun, S., & Park, J. I. (2013). Dyrk2-associated EDD-DDB1-VprBP E3 Ligase Inhibits Telomerase by TERT Degradation. *Journal of Biological Chemistry*, *288*(10), 7252-7262. https://doi.org/10.1074/jbc.M112.416792

Kang, S. S., Kwon, T., & Do, S. I. (1999). Akt protein kinase enhances human telomerase activity through phosphorylation of telomerase reverse transcriptase subunit. *Journal of Biological Chemistry*, *274*(19), 13085-13090.

Kennedy, P. G. (2013). Clinical features, diagnosis, and treatment of human African trypanosomiasis (sleeping sickness). *The Lancet Neurology*, *12*(2), 186-194.

Kharbanda, S., Kumar, V., Dhar, S., Pandey, P., Chen, C., Majumder, P., Yuan, Z., Whang, Y., Strauss, W., & Pandita, T. K. (2000). Regulation of the hTERT telomerase catalytic subunit by the c-Abl tyrosine kinase. *Current Biology*, *10*(10), 568-575.

Kim, J. H., Park, S.-M., Kang, M. R., Oh, S.-Y., Lee, T. H., Muller, M. T., & Chung, I. K. (2005). Ubiquitin ligase MKRN1 modulates telomere length homeostasis through a proteolysis of hTERT. *Genes & development*, *19*(7), 776-781.

Kim, N.-K., Zhang, Q., & Feigon, J. (2014). Structure and sequence elements of the CR4/5 domain of medaka telomerase RNA important for telomerase function. *Nucleic acids research*, *42*(5), 3395-3408.

Klebanov-Akopyan, O., Mishra, A., Glousker, G., Tzfati, Y., & Shlomai, J. (2018). Trypanosoma brucei UMSBP2 is a single-stranded telomeric DNA binding protein essential for chromosome end protection. *Nucleic acids research*, *46*(15), 7757-7771. https://doi.org/10.1093/nar/gky597

Krissinel, E., & Henrick, K. (2004). Secondary-structure matching (SSM), a new tool for fast protein structure alignment in three dimensions. *Acta Crystallographica Section D-Structural Biology*, *60*, 2256-2268. https://doi.org/10.1107/S0907444904026460

Kumar, S., Stecher, G., Li, M., Knyaz, C., & Tamura, K. (2018). MEGA X: molecular evolutionary genetics analysis across computing platforms. *Molecular biology and evolution*, *35*(6), 1547.

Lemieux, B., Laterreur, N., Perederina, A., Noël, J.-F., Dubois, M.-L., Krasilnikov, A. S., & Wellinger, R. J. (2016). Active yeast telomerase shares subunits with ribonucleoproteins RNase P and RNase MRP. *Cell*, *165*(5), 1171-1181.

Lin, K. W., McDonald, K. R., Guise, A. J., Chan, A., Cristea, I. M., & Zakian, V. A. (2015). Proteomics of yeast telomerase identified Cdc48-Npl4-Ufd1 and Ufd4 as regulators of Est1 and telomere length. *Nature Communications*, *6*. https://doi.org/ARTN 8290
10.1038/ncomms9290

Logeswaran, D., Li, Y., Podlevsky, J. D., & Chen, J. J.-L. (2021). Monophyletic origin and divergent evolution of animal telomerase RNA. *Molecular biology and evolution*, *38*(1), 215-228.

Marcand, S. (2014). How do telomeres and NHEJ coexist? *Molecular & cellular oncology*, *1*(3), e963438.

Mason, D. X., Goneska, E., & Greider, C. W. (2003). Stem-loop IV of tetrahymena telomerase RNA stimulates processivity in trans. *Molecular and cellular biology*, *23*(16), 5606-5613.

Masutomi, K., Kaneko, S., Hayashi, N., Yamashita, T., Shirota, Y., Kobayashi, K., & Murakami, S. (2000). Telomerase activity reconstituted in vitro with purified human telomerase reverse transcriptase and human telomerase RNA component. *Journal of Biological Chemistry*, *275*(29), 22568-22573.

Mitchell, J. R., & Collins, K. (2000). Human telomerase activation requires two independent interactions between telomerase RNA and telomerase reverse transcriptase. *Molecular Cell*, *6*(2), 361-371. https://doi.org/Doi 10.1016/S1097-2765(00)00036-8

Mochizuki, Y., He, J., Kulkarni, S., Bessler, M., & Mason, P. J. (2004). Mouse dyskerin mutations affect accumulation of telomerase RNA and small nucleolar RNA, telomerase activity, and ribosomal RNA processing. *Proceedings of the National Academy of Sciences of the United States of America*, *101*(29), 10756-10761. https://doi.org/10.1073/pnas.0402560101

Moon, D. H., Segal, M., Boyraz, B., Guinan, E., Hofmann, I., Cahan, P., Tai, A. K., & Agarwal, S. (2015). Poly(A)-specific ribonuclease (PARN) mediates 3 '-end maturation of the telomerase RNA component. *Nature Genetics*, *47*(12), 1482-+. https://doi.org/10.1038/ng.3423

Nanavaty, V., Sandhu, R., Jehi, S. E., Pandya, U. M., & Li, B. B. (2017). Trypanosoma brucei RAP1 maintains telomere and subtelomere integrity by suppressing TERRA and telomeric RNA: DNA hybrids. *Nucleic acids research*, *45*(10), 5785-5796. https://doi.org/10.1093/nar/gkx184

Nguyen, T. H. D., Tam, J., Wu, R. A., Greber, B. J., Toso, D., Nogales, E., & Collins, K. (2018). Cryo-EM structure of substrate-bound human telomerase holoenzyme. *Nature*, *557*(7704), 190-195.

Nittis, T., Guittat, L., LeDuc, R. D., Dao, B., Duxin, J. P., Rohrs, H., Townsend, R. R., & Stewart, S. A. (2010). Revealing Novel Telomere Proteins Using in Vivo Cross-linking, Tandem Affinity Purification, and Label-free Quantitative LC-FTICR-MS. *Molecular & Cellular Proteomics*, *9*(6), 1144-1156. https://doi.org/10.1074/mcp.M900490-MCP200

Orsburn, B. C. (2021). Proteome discoverer—a community enhanced data processing suite for protein informatics. *Proteomes*, *9*(1), 15.

Peters, J. M. (2006). The anaphase promoting complex/cyclosome: a machine designed to destroy. *Nature reviews Molecular cell biology*, *7*(9), 644-656. https://doi.org/10.1038/nrm1988

Podlevsky, J. D., Li, Y., & Chen, J. J.-L. (2016). The functional requirement of two structural domains within telomerase RNA emerged early in eukaryotes. *Nucleic acids research*, *44*(20), 9891-9901.

Qi, X., Li, Y., Honda, S., Hoffmann, S., Marz, M., Mosig, A., Podlevsky, J. D., Stadler, P. F., Selker, E. U., & Chen, J. J.-L. (2013). The common ancestral core of vertebrate and fungal telomerase RNAs. *Nucleic acids research*, *41*(1), 450-462.

Rabbani, M. A. G., Tonini, M. L., Afrin, M., & Li, B. B. (2022). POLIE suppresses telomerase-mediated telomere G-strand extension and helps ensure proper telomere C-strand synthesis in trypanosomes. *Nucleic acids research*, *50*(4), 2036-2050. https://doi.org/10.1093/nar/gkac023

Ree, R., Varland, S., & Arnesen, T. (2018). Spotlight on protein N-terminal acetylation. *Experimental & molecular medicine*, *50*(7), 1-13.

Respuela, P., Ferella, M., Rada-Iglesias, A., & Åslund, L. (2008). Histone acetylation and methylation at sites initiating divergent polycistronic transcription in Trypanosoma cruzi. *Journal of Biological Chemistry*, *283*(23), 15884-15892.

Richards, R. J., Theimer, C. A., Finger, L. D., & Feigon, J. (2006). Structure of the Tetrahymena thermophila telomerase RNA helix II template boundary element. *Nucleic acids research*, *34*(3), 816-825.

Roake, C. M., & Artandi, S. E. (2020). Regulation of human telomerase in homeostasis and disease. *Nature reviews Molecular cell biology*, *21*(7), 384-397. https://doi.org/10.1038/s41580-020-0234-z

Robart, A. R., & Collins, K. (2010). Investigation of human telomerase holoenzyme assembly, activity, and processivity using disease-linked subunit variants. *Journal of Biological Chemistry*, *285*(7), 4375-4386.

Rymond, B. C. (1993). Convergent transcripts of the yeast PRP38-SMD1 locus encode two essential splicing factors, including the D1 core polypeptide of small nuclear ribonucleoprotein particles. *Proceedings of the National Academy of Sciences*, *90*(3), 848-852.

Saha, A., Nanavaty, V. P., & Li, B. B. (2020). Telomere and Subtelomere R-loops and Antigenic Variation in Trypanosomes. *Journal of Molecular Biology*, *432*(15), 4167-4185. https://doi.org/10.1016/j.jmb.2019.10.025

Sandhu, R., Sanford, S., Basu, S., Park, M., Pandya, U. M., Li, B., & Chakrabarti, K. (2013). A trans-spliced telomerase RNA dictates telomere synthesis in Trypanosoma brucei. *Cell research*, *23*(4), 537-551.

Santos, J. H., Meyer, J. N., Skorvaga, M., Annab, L. A., & Van Houten, B. (2004). Mitochondrial hTERT exacerbates free-radical-mediated mtDNA damage. *Aging Cell*, *3*(6), 399-411. https://doi.org/10.1111/j.1474-9728.2004.00124.x

Schuberth, C., Richly, H., Rumpf, S., & Buchberger, A. (2004). Shp1 and Ubx2 are adaptors of Cdc48 involved in ubiquitin-dependent protein degradation. *Embo Reports*, *5*(8), 818-824. https://doi.org/10.1038/sj.embor.7400203

Sealey, D. C. F., Kostic, A. D., Lebel, C., Pryde, F., & Harrington, L. (2011). The TPR-containing domain within Est1 homologs exhibits species-specific roles in telomerase interaction and telomere length homeostasis. *Bmc Molecular Biology*, *12*. https://doi.org/Artn 45

10.1186/1471-2199-12-45

Sharanov, Y. S., Zvereva, M., & Dontsova, O. (2006). Saccharomyces cerevisiae telomerase subunit Est3p binds DNA and RNA and stimulates unwinding of RNA/DNA heteroduplexes. *FEBS letters*, *580*(19), 4683-4690.

Sharma, N. K., Reyes, A., Green, P., Caron, M. J., Bonini, M. G., Gordon, D. M., Holt, I. J., & Santos, J. H. (2012). Human telomerase acts as a hTR-independent reverse transcriptase in mitochondria. *Nucleic acids research*, *40*(2), 712-725. https://doi.org/10.1093/nar/gkr758

Shay, J. W., & Wright, W. E. (2019). Telomeres and telomerase: three decades of progress. *Nature Reviews Genetics*, *20*(5), 299-309.

Simpson, L., Thiemann, O. H., Savill, N. J., Alfonzo, J. D., & Maslov, D. (2000). Evolution of RNA editing in trypanosome mitochondria. *Proceedings of the National Academy of Sciences*, *97*(13), 6986-6993.

Singh, M., Wang, Z. H., Koo, B. K., Patel, A., Cascio, D., Collins, K., & Feigon, J. (2012). Structural Basis for Telomerase RNA Recognition and RNP Assembly by the Holoenzyme La Family Protein p65. *Molecular Cell*, *47*(1), 16-26. https://doi.org/10.1016/j.molcel.2012.05.018

Song, J., Logeswaran, D., Castillo-González, C., Li, Y., Bose, S., Aklilu, B. B., Ma, Z., Polkhovskiy, A., Chen, J. J.-L., & Shippen, D. E. (2019). The conserved structure of plant telomerase RNA provides the missing link for an evolutionary pathway from

ciliates to humans. *Proceedings of the National Academy of Sciences*, *116*(49), 24542-24550.

Stellwagen, A. E., Haimberger, Z. W., Veatch, J. R., & Gottschling, D. E. (2003). Ku interacts with telomerase RNA to promote telomere addition at native and broken chromosome ends. *Genes & development*, *17*(19), 2384-2395.

Steverding, D. (2017). Sleeping sickness and nagana disease caused by Trypanosoma brucei. *Arthropod borne diseases*, 277-297.

Sutton, R. E., & Boothroyd, J. C. (1986). Evidence for trans splicing in trypanosomes. *Cell*, *47*(4), 527-535.

Tang, W., Kannan, R., Blanchette, M., & Baumann, P. (2012). Telomerase RNA biogenesis involves sequential binding by Sm and Lsm complexes. *Nature*, *484*(7393), 260-U152. https://doi.org/10.1038/nature10924

te Raa, G. D., Derks, I. A. M., Navrkalova, V., Skowronska, A., Moerland, P. D., van Laar, J., Oldreive, C., Monsuur, H., Trbusek, M., Malcikova, J., Loden, M., Geisler, C. H., Hullein, J., Jethwa, A., Zenz, T., Pospisilova, S., Stankovic, T., van Oers, M. H. J., Kater, A. P., & Eldering, E. (2015). The impact of SF3B1 mutations in CLL on the DNA-damage response. *Leukemia*, *29*(5), 1133-1142. https://doi.org/10.1038/leu.2014.318

Tian, L. L., & Weizmann, Y. (2013). Real-Time Detection of Telomerase Activity Using the Exponential Isothermal Amplification of Telomere Repeat Assay. *Journal of the American Chemical Society*, *135*(5), 1661-1664. https://doi.org/10.1021/ja309198j

Tran, N. H., Qiao, R., Xin, L., Chen, X., Liu, C., Zhang, X., Shan, B., Ghodsi, A., & Li, M. (2019). Deep learning enables de novo peptide sequencing from data-independent-acquisition mass spectrometry. *Nature Methods*, *16*(1), 63-66.

Tyanova, S., Temu, T., Sinitcyn, P., Carlson, A., Hein, M. Y., Geiger, T., Mann, M., & Cox, J. (2016). The Perseus computational platform for comprehensive analysis of (prote)omics data. *Nature Methods*, *13*(9), 731-740. https://doi.org/10.1038/Nmeth.3901

Upton, H. E., Chan, H., Feigon, J., & Collins, K. (2017). Shared Subunits of Tetrahymena Telomerase Holoenzyme and Replication Protein A Have Different Functions in Different Cellular Complexes. *Journal of Biological Chemistry*, *292*(1), 217-228. https://doi.org/10.1074/jbc.M116.763664

Vasconcelos, E. J. R., Nunes, V. S., da Silva, M. S., Segatto, M., Myler, P. J., & Cano, M. I. N. (2014). The Putative Leishmania Telomerase RNA (LeishTER) Undergoes Trans-Splicing and Contains a Conserved Template Sequence. *Plos One*, *9*(11). https://doi.org/ARTN e112061
10.1371/journal.pone.0112061

Vasianovich, Y., Bajon, E., & Wellinger, R. J. (2020). Telomerase biogenesis requires a novel Mex67 function and a cytoplasmic association with the Sm7 complex. *Elife*, *9*, e60000.

Venteicher, A. S., Abreu, E. B., Meng, Z., McCann, K. E., Terns, R. M., Veenstra, T. D., Terns, M. P., & Artandi, S. E. (2009). A human telomerase holoenzyme protein required for Cajal body localization and telomere synthesis. *Science*, *323*(5914), 644-648.

Venteicher, A. S., Meng, Z. J., Mason, P. J., Veenstra, T. D., & Artandi, S. E. (2008). Identification of ATPases pontin and reptin as telomerase components essential for holoenzyme assembly. *Cell*, *132*(6), 945-957. https://doi.org/10.1016/j.cell.2008.01.019

Vulliamy, T., Marrone, A., Goldman, F., Dearlove, A., Bessler, M., Mason, P. J., & Dokal, I. (2001). The RNA component of telomerase is mutated in autosomal dominant dyskeratosis congenita. *Nature*, *413*(6854), 432-435.

Wang, L. L., Brooks, A. N., Fan, J., Wan, Y. Z., Gambe, R., Li, S. Q., Hergert, S., Yin, S. Y., Freeman, S. S., Levin, J. Z., Fan, L., Seiler, M., Buonamici, S., Smith, P. G., Chau, K. F., Cibulskis, C. L., Zhang, W. D., Rassenti, L. Z., Ghia, E. M., . . . Wu, C. J. (2016). Transcriptomic Characterization of SF3B1 Mutation Reveals Its Pleiotropic Effects in Chronic Lymphocytic Leukemia. *Cancer Cell*, *30*(5), 750-763. https://doi.org/10.1016/j.ccell.2016.10.005

Wang, Y., Sušac, L., & Feigon, J. (2019). Structural biology of telomerase. *Cold Spring Harbor perspectives in biology*, *11*(12), a032383.

Watkins, N. J., & Bohnsack, M. T. (2012). The box C/D and H/ACA snoRNPs: key players in the modification, processing and the dynamic folding of ribosomal RNA. *Wiley Interdisciplinary Reviews: RNA*, *3*(3), 397-414.

Welburn, S. C., Fèvre, E. M., Coleman, P. G., Odiit, M., & Maudlin, I. (2001). Sleeping sickness: a tale of two diseases. *Trends in parasitology*, *17*(1), 19-24.

Wirtz, E., Leal, S., Ochatt, C., & Cross, G. A. M. (1999). A tightly regulated inducible expression system for conditional gene knock-outs and dominant-negative genetics in Trypanosoma brucei. *Molecular and Biochemical Parasitology*, *99*(1), 89-101. https://doi.org/Doi 10.1016/S0166-6851(99)00002-X

Witkin, K. L., & Collins, K. (2004). Holoenzyme proteins required for the physiological assembly and activity of telomerase. *Genes & development*, *18*(10), 1107-1118. https://doi.org/10.1101/gad.1201704

Xie, M., Mosig, A., Qi, X., Li, Y., Stadler, P. F., & Chen, J. J.-L. (2008). Structure and function of the smallest vertebrate telomerase RNA from teleost fish. *Journal of Biological Chemistry*, *283*(4), 2049-2059.

Xin, H., Liu, D., & Songyang, Z. (2008). The telosome/shelterin complex and its functions. *Genome biology*, *9*(9), 1-7.

Yang, X. F., Figueiredo, L. M., Espinal, A., Okubo, E., & Li, B. (2009). RAP1 Is Essential for Silencing Telomeric Variant Surface Glycoprotein Genes in Trypanosoma brucei. *Cell*, *137*(1), 99-109. https://doi.org/10.1016/j.cell.2009.01.037

Yin, Q.-F., Yang, L., Zhang, Y., Xiang, J.-F., Wu, Y.-W., Carmichael, G. G., & Chen, L.-L. (2012). Long noncoding RNAs with snoRNA ends. *Molecular Cell*, *48*(2), 219-230.

Zhang, N., Jiang, N., Yu, L., Guan, T., Sang, X., Feng, Y., Chen, R., & Chen, Q. (2021). Protein lactylation critically regulates energy metabolism in the protozoan parasite Trypanosoma brucei. *Frontiers in Cell and Developmental Biology*, *9*, 719720.

Zhang, N., Jiang, N., Zhang, K., Zheng, L., Zhang, D., Sang, X., Feng, Y., Chen, R., Yang, N., & Wang, X. (2020). Landscapes of protein posttranslational modifications of African Trypanosoma parasites. *Iscience*, *23*(5), 101074.

Zhou, J., Hidaka, K., & Futcher, B. (2000). The Est1 subunit of yeast telomerase binds the Tlc1 telomerase RNA. *Molecular and cellular biology*, *20*(6), 1947-1955.